© 2020. Published by The Company of Biologists Ltd | Development (2020) 147, dev186551. doi:10.1242/dev.186551

RESEARCH ARTICLE

# Assisted reproductive technologies induce temporally specific placental defects and the preeclampsia risk marker sFLT1 in mouse

**Lisa A. Vrooman[1], Eric A. Rhon-Calderon[1], Olivia Y. Chao[1], Duy K. Nguyen[1], Laren Narapareddy[1,2], Asha K. Dahiya[1], Mary E. Putt[3], Richard M. Schultz[4] and Marisa S. Bartolomei[1,*]**

## ABSTRACT

Although widely used, assisted reproductive technologies (ARTs) are associated with adverse perinatal outcomes. To elucidate their underlying causes, we have conducted a longitudinal analysis of placental development and fetal growth using a mouse model to investigate the effects of individual ART procedures: hormone stimulation, *in vitro* fertilization (IVF), embryo culture and embryo transfer. We demonstrate that transfer of blastocysts naturally conceived without hormone stimulation and developed *in vivo* prior to transfer can impair early placentation and fetal growth, but this effect normalizes by term. In contrast, embryos cultured *in vitro* before transfer do not exhibit this compensation but rather display placental overgrowth, reduced fetal weight, reduced placental DNA methylation and increased levels of sFLT1, an anti-angiogenic protein implicated in causing the maternal symptoms of preeclampsia in humans. Increases in sFLT1 observed in this study suggest that IVF procedures could increase the risk for preeclampsia. Moreover, our results indicate that embryo culture is the major factor contributing to most placental abnormalities and should therefore be targeted for optimization.

**KEY WORDS: Assisted reproductive technologies, Fetal growth, Placenta, Preeclampsia, sFLT1**

## INTRODUCTION

Assisted reproductive technologies (ARTs), including *in vitro* fertilization (IVF), have enabled the birth of over 8 million babies worldwide (Adamson et al., 2012). ART use has become more common in recent years with the number of ART cycles increasing 30% over the past decade in the USA (Centers for Disease Control and Prevention et al., 2017). In Europe and Asia, ART use is much higher (Dyer et al., 2016). Studies of human singleton pregnancies demonstrate that ART is associated with abnormal placentation, preeclampsia, small- and large-for-gestational age babies, preterm birth, miscarriage, perinatal mortality, pregnancy complications, and congenital disorders (Daniel et al., 1999; Haavaldsen et al., 2012; Luke et al., 2017, 2019; Marino et al., 2014; Pandey et al., 2012; Schieve et al., 2007; Stern et al., 2018; Wisborg et al., 2010). Although the underlying infertility/subfertility of patients can contribute to these risks (e.g. Hwang et al., 2018; Kobayashi et al., 2009), numerous studies using fertile animal models suggest ART procedures alone can induce fetal and placental growth changes, and that these changes can result in different outcomes dependent on culture conditions, genetic background and stage of embryo transfer, among other variables (Bloise et al., 2014). In mouse, IVF concepti display placental overgrowth and small- and large-for-gestational age offspring, outcomes also observed in some human IVF pregnancies (Bloise et al., 2012; Chen et al., 2015a,b; Collier et al., 2009; de Waal et al., 2015; Sui et al., 2014; Tan et al., 2016).

The placenta is essential for pregnancy. In addition to its nutrient and gas transport function, the placenta also plays important endocrine, metabolic, immunoprotective, sequestration and barrier roles (Maltepe and Fisher, 2015). Placenta dysfunction restricts fetal growth and can lead to adverse health outcomes in adulthood (Gagnon, 2003; Maltepe and Fisher, 2015), making it imperative to understand how factors, such as IVF, impair placentation. More recent clinical reports demonstrate the risk of placenta previa, placental abruption and morbidly adherent placenta is two to four times higher in ART singletons when compared with naturally conceived singletons (Vermey et al., 2018). The risk of placenta accreta, a form of morbidly adherent placenta, may be as much as 13 times higher in ART pregnancies (Esh-Broder et al., 2011). Although maternal risk factors play a clear role in the risk of placenta accreta, embryo culture, as well as cryopreservation, are postulated to be contributing factors (Esh-Broder et al., 2011; Kaser et al., 2015). There is also strong clinical evidence that ART pregnancies are at greater risk of preeclampsia, a pregnancy complication with known placental etiology (Di Tommaso et al., 2019; Luke et al., 2019; Pandey et al., 2012; Thomopoulos et al., 2017; von Versen-Höynck et al., 2019). It is unknown whether and how ART procedures induce placental defects specific to these clinically relevant conditions and which procedures need to be optimized to ameliorate adverse outcomes. Given that these specific conditions are life-threatening for both mother and fetus and may predispose offspring to adverse long-term health outcomes, lowering the risk of these ART-associated placental abnormalities is a major health need.

We and others have previously identified both overgrowth and epigenetic changes in term placentas of mice generated by IVF (Chen et al., 2015a; de Waal et al., 2015; Sui et al., 2014). The goal of the

[1]Epigenetics Institute, Department of Cell and Developmental Biology, Perelman School of Medicine, University of Pennsylvania, Philadelphia, PA 19104, USA. [2]Department of Family and Community Health, Claire M. Fagin School of Nursing, University of Pennsylvania, Philadelphia, PA 19104, USA. [3]Department of Biostatistics, Epidemiology, and Informatics, Perelman School of Medicine, University of Pennsylvania, Philadelphia, PA 19104, USA. [4]Department of Biology, School of Arts and Sciences, University of Pennsylvania, Philadelphia, PA 19104, USA.

*Author for correspondence (bartolom@pennmedicine.upenn.edu)

L.A.V., 0000-0002-2202-1051; E.A.R.-C., 0000-0001-8128-724X; D.K.N., 0000-0002-2312-2567; L.N., 0000-0002-3327-4089; M.E.P., 0000-0001-7954-1288; R.M.S., 0000-0001-5923-6825; M.S.B., 0000-0001-9410-5222

**Handling Editor: Patrick Tam**
**Received 16 November 2019; Accepted 18 April 2020**

Development (2020) 147, dev186551. doi:10.1242/dev.186551

present study was to assess the effect of specific ART procedures on eliciting placental abnormalities and determine which procedures need to be optimized to ameliorate these abnormalities. Furthermore, we hypothesized that impaired placental development is due to underlying epigenetic perturbations incurred specifically during embryo culture. Accordingly, we conducted a detailed developmental analysis of naturally conceived and ART procedure concepti, controlling for individual ART procedures: hormone stimulation, IVF, embryo culture and embryo transfer. We assessed concepti shortly after placental formation at embryonic day (E) 12.5, when the placenta reaches maximal growth and fetal weight begins to increase exponentially at E14.5, and at term: E18.5. Unexpectedly, at mid-gestation, we found embryo transfer alone led to both impaired placental vasculature and reduced fetal weight; improvement in fetal weight and placental vasculature was subsequently observed by term. Importantly, the worst fetal and placental outcomes were specifically linked to embryo culture under current state-of-the-art conditions. Concepti derived from transferred cultured embryos failed to achieve normal fetal weight by term and were found to have placental abnormalities reflective of placental overgrowth and preeclampsia – abnormalities observed in human ART pregnancies. Importantly, all these phenotypes were linked to loss of placental DNA methylation, which suggests underlying epigenetic perturbations incurred during embryo culture cause late gestational placental abnormalities and impair placental compensatory mechanisms.

## RESULTS

### ART procedures result in reduced fetal weight preceding placental overgrowth

We first compared the effect of different ART procedures on fetal and placental weight; see Materials and Methods for experimental design, Table S1 for nomenclature for different procedures and Table S2 for litter characteristics. Unexpectedly, at E12.5, mean fetal weight was significantly reduced in embryo transfer (ET), hormone stimulation (S), embryo culture (EC) and *in vitro* fertilization (IVF) groups when compared with naturally conceived controls (Fig. 1A). At E14.5, when compared with naturally conceived controls, mean fetal weight remained significantly reduced in S, EC and IVF, but not in ET (Fig. 1B). A mouse fetus normally experiences exponential growth from

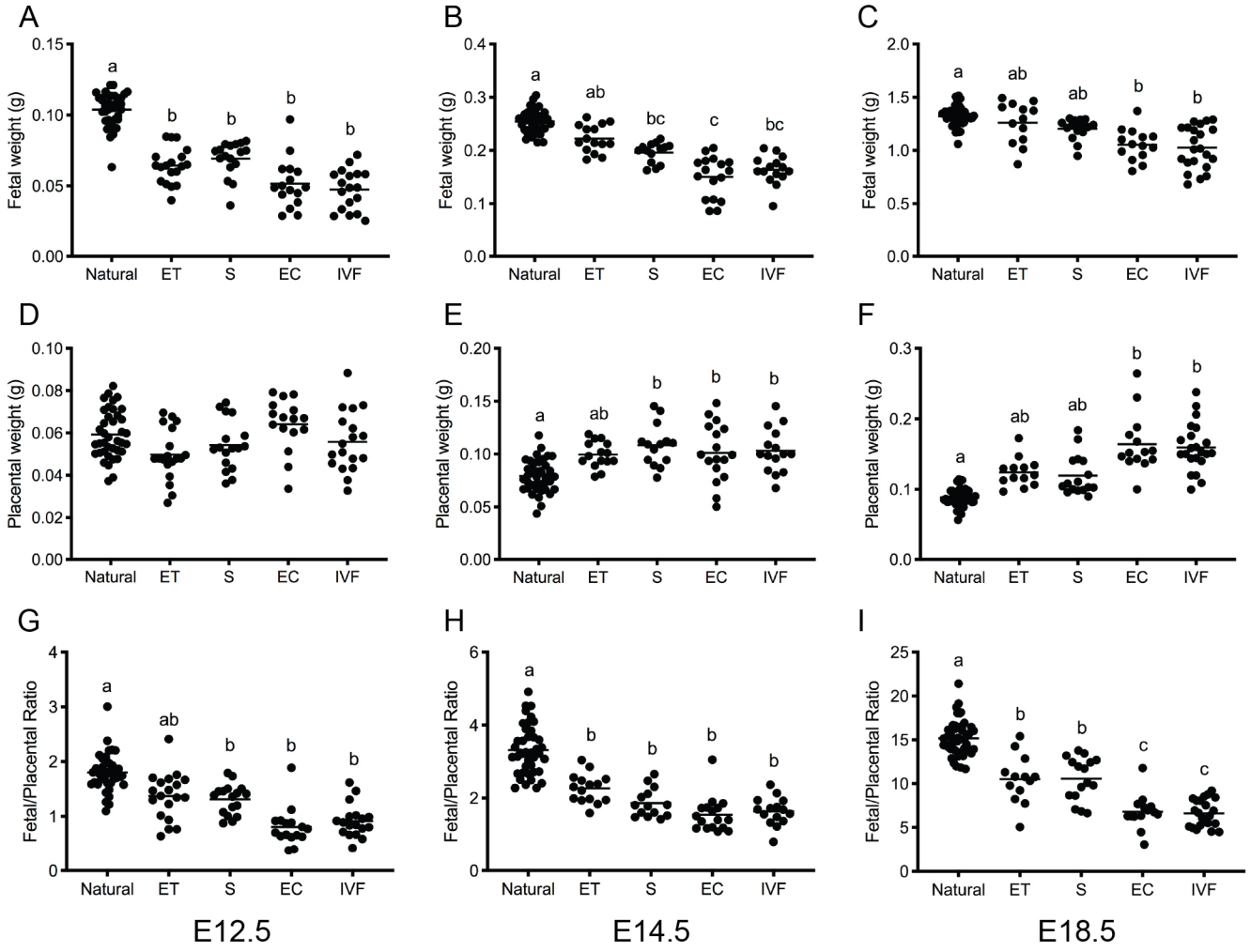


**Fig. 1. Fetal weight, placental weight and fetal:placental ratios in a mouse model of IVF procedures at E12.5, E14.5 and E18.5.** (A-I) Each data point represents an individual conceptus from a minimum of three different litters ($n$=13-21 per group for ART groups, $n$=46-54 per group for natural control groups). Black line represents the mean of each group. A significant ($P$<0.05) global likelihood ratio test of differences between groups in the mixed effects model was followed by pairwise tests adjusted using a Holm-Bonferroni correction. Groups with different letters indicate significant differences between groups (adjusted $P$<0.05); the same letters indicate no difference was detected. For E14.5 placental weight, raw $P$-values were used to infer pairwise among experimental groups, acknowledging that the use of raw $P$-values does not strictly control the family-wise type I error rate.

Development (2020) 147, dev186551. doi:10.1242/dev.186551

E14.5 to term (Mu et al., 2008) and all groups displayed this dramatic increase in fetal weight (Fig. S1A-E). By E18.5, S mean fetal weight was similar to naturally conceived controls, whereas EC and IVF mean fetal weights remained significantly lower (Fig. 1C).

In contrast to fetal weight, mean placental weight did not differ among any of the groups at E12.5 (Fig. 1D). By E14.5, however, S, EC and IVF placentas were significantly larger than placentas from naturally conceived mice (Fig. 1E). Placental growth normally plateaus around E14.5 (Mu et al., 2008), which we observed in placentas from naturally conceived mice (Fig. S1F). In contrast, placental weight continued to increase in ART groups in ET, S, EC and IVF groups when compared with naturally conceived controls at E18.5 (Fig. 1F, Fig. S1G-J). The reduction in fetal weight and concomitant increase in placental weight resulted in significantly reduced fetal/placental weight ratios, a rough measure of placental efficiency, for the ET group at E14.5 and E18.5, and for S, EC and IVF groups at all three developmental time points (Fig. 1G-I). Notably, EC and IVF groups had the most drastic differences in fetal and placental weight, and were not statistically different from each other. These weight trends were similar when statistically compared by litter mean, with the exception of S and EC fetal weight, which were no longer statistically different from natural controls at E18.5 (Fig. S2). Males and females were equally affected by ART procedures (Fig. S3). These results suggest that: (1) factors related to embryo transfer can impair early fetal growth shortly after placental formation; (2) the ET group can undergo late gestational compensatory fetal growth; and (3) embryo culture induces the most drastic increase in placental weight in late gestation associated with impaired fetal growth.

### Labyrinth abnormalities are detected in ART embryos at mid-gestation, shortly after placental formation

The mouse placenta consists of two main tissue types: the labyrinth, containing the maternal and fetal vasculature for nutrient and gas exchange; and the junctional zone, which serves primarily an endocrine function (Simmons, 2014). Given the striking difference in fetal weight observed in all ART groups at E12.5, we assessed a subset of placentas for labyrinth defects using immunohistochemistry for CD34, which is a marker of fetal blood vessel endothelial cells. We observed qualitative differences in ET, S, EC and IVF E12.5 placentas with respect to blood vessel density and organization (Fig. 2A-E). Quantitative image analyses showed a significant reduction in CD34-positive staining, which is indicative of fewer fetal blood vessels, in EC E12.5 placentas when compared with natural controls (Fig. 2F). By E14.5, no ART groups were statistically different from natural controls, but S placentas had significantly higher CD34-positive area relative to labyrinth area than the EC group (Fig. 2G). By E18.5, no significant differences were observed between any of the groups (Fig. 2H), although some individual EC and IVF placentas displayed abnormal blood vessel organization in focal areas of the labyrinth (Fig. S4).

To assess labyrinth trophoblast cells, we used expression of *Ctsq*, *Slc16a1* and *Slc16a3*, as cell type-specific markers of sinusoidal trophoblast giant cells, syncytiotrophoblast layer I and

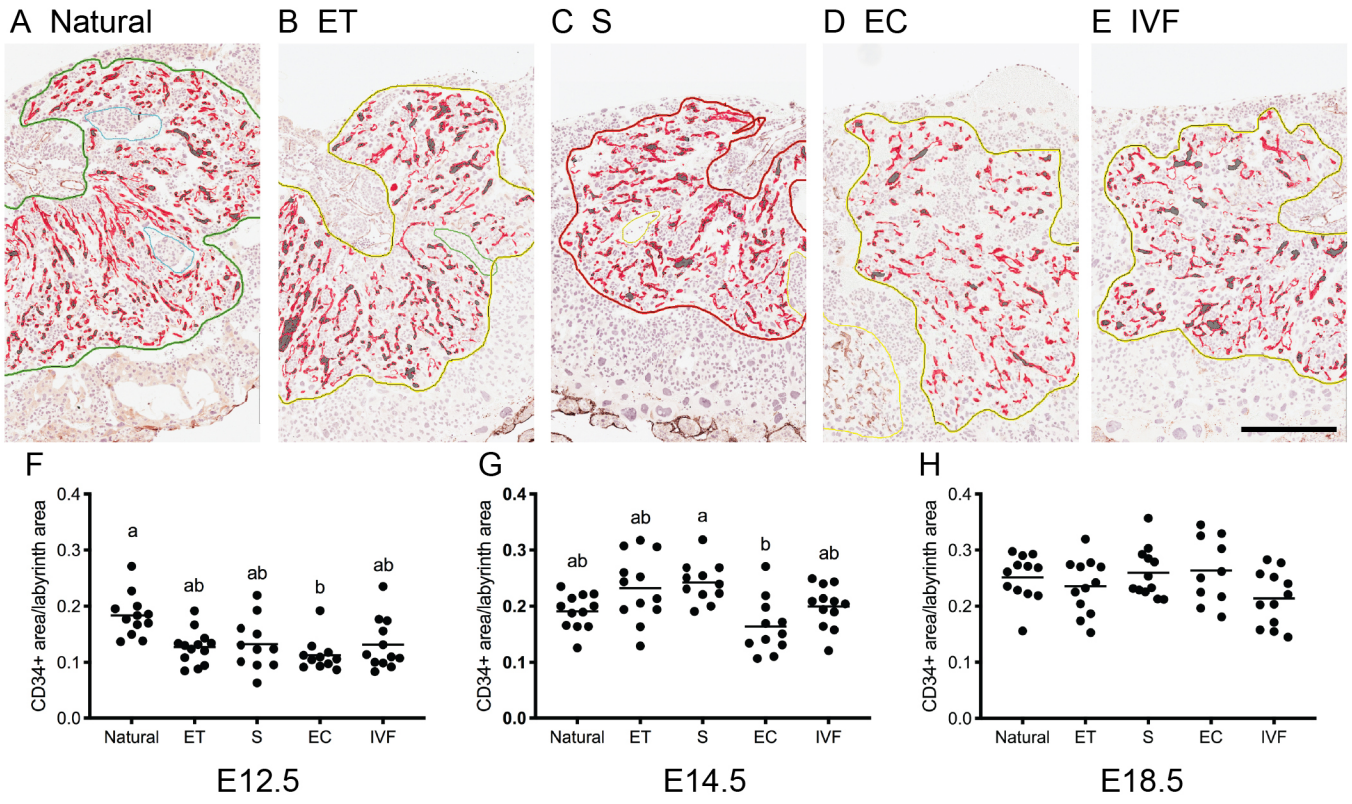


**Fig. 2. Qualitative and quantitative labyrinth fetal endothelial cell analyses in a mouse model of IVF procedures at E12.5, E14.5 and E18.5.** (A-E) CD34 immunostaining counterstained with Hematoxylin was used to visualize fetal endothelial cells. Representative images of labyrinth from (A) natural, (B) ET, (C) S, (D) EC and (E) IVF placentas at E12.5. Scale bar: 300 µm. (F-H) Fetal endothelial cell positive staining (shown here, false colored in red) was analyzed as a percentage of total labyrinth area using ePathology software. Each data point represents an individual conceptus from a minimum of three different litters ($n$=10-13/group). A significant ($P$<0.05) global likelihood ratio test of differences between groups in the mixed effects model was followed by pairwise tests adjusted using a Holm-Bonferroni correction. Groups with different letters indicate significant differences between groups (adjusted $P$<0.05); similar letters indicate no difference was detected.

Development (2020) 147, dev186551. doi:10.1242/dev.186551

syncytiotrophoblast layer II cells, respectively. At E12.5, expression of *Ctsq* was significantly reduced in all ART groups when compared with controls (Fig. 3A,G), whereas *Slc16a1* was significantly reduced only in EC and IVF (Fig. 3D), and *Slc16a3* was significantly reduced in S, EC and IVF. At E14.5 and E18.5, expression of *Slc16a1* was no longer statistically different among groups. For *Slc16a3* expression, significant differences were observed only between the S and IVF group at E14.5, whereas at E18.5 significant differences were only observed between the IVF group and natural, ET and S group (Fig. 3E, F,H,I). Significant reduction in *Ctsq* expression was detected only in the EC group when compared with naturals at E14.5 (Fig. 3B), but at E18.5, the IVF group had significantly reduced *Ctsq* expression when compared with natural and ET groups (Fig. 3C). Thus, with the exception of sinusoidal trophoblast giant cells, both the histological and molecular labyrinth phenotype of the ART groups improved during development.

### Junctional zone overgrowth is observed in late gestation

IVF placentas have an over-representation of junctional zone at term (Chen et al., 2015a; de Waal et al., 2015; Sui et al., 2014). To better understand how junctional zone overgrowth occurs during placenta development, we used an *in situ* hybridization probe for *Tpbpa*, a junctional zone marker (Fig. 4). No differences in gross morphology, junctional zone area, labyrinth area or the percentage of the two tissues were detected among all groups at E12.5 (Figs 4 and 5A,D). At E14.5, finger-like projections of the junctional zone into the labyrinth could be observed in S, EC and IVF placentas (Fig. 4), even though junctional zone area, labyrinth area or the percentage of the two tissues were not significantly different (Fig. 5B,E). By E18.5, junctional zone area and the percentage of junctional zone were significantly higher in EC and IVF placentas compared with controls (Figs 4 and 5C,I). The border between the junctional zone and labyrinth tissues, which are characteristic of term placentas, was less distinct in some EC and IVF placentas, suggesting changes in cell proliferation and migration (Fig. S4C).

We used a *Prl8a8 in situ* hybridization probe, which is specific to spongiotrophoblasts, and the distinct morphology of glycogen cell and parietal trophoblast giant cells (P-TGCs) to determine whether the junctional zone cell types contributed proportionally to the late gestational junctional zone overgrowth. There was no difference in P-TGCs at E12.5, but by E14.5, EC and IVF groups had proportionally more P-TGCs than natural or ET placentas

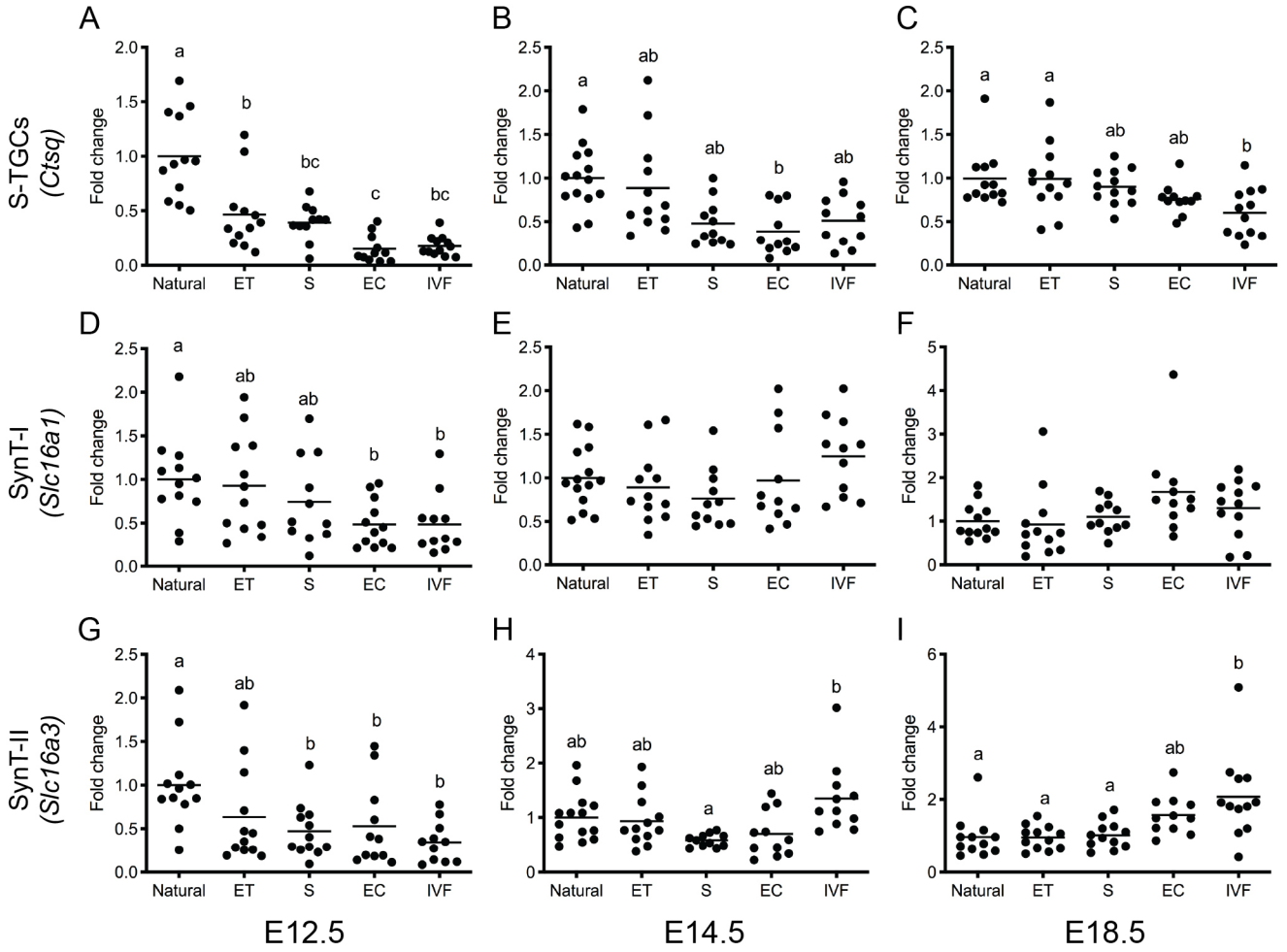


**Fig. 3. Gene expression of labyrinth trophoblast cell markers in a mouse model of IVF procedures at E12.5, E14.5 and E18.5.** (A-I) Each data point represents an individual placenta from a minimum of three different litters ($n$=10-13 per group). Black line represents the mean of each group. A significant ($P$<0.05) global likelihood ratio test of differences between groups in the mixed effects model was followed by pairwise tests adjusted using a Holm-Bonferroni correction. Groups with different letters indicate significant differences between groups (adjusted $P$<0.05); the same letters indicate no difference was detected. For E12.5 *Slc16a1*, E12.5 *Slc16a3* and E14.5 *Slc16a3*, raw $P$-values were used to infer pairwise differences among experimental groups, acknowledging that the use of raw $P$-values does not strictly control the family-wise type I error rate.

Development (2020) 147, dev186551. doi:10.1242/dev.186551

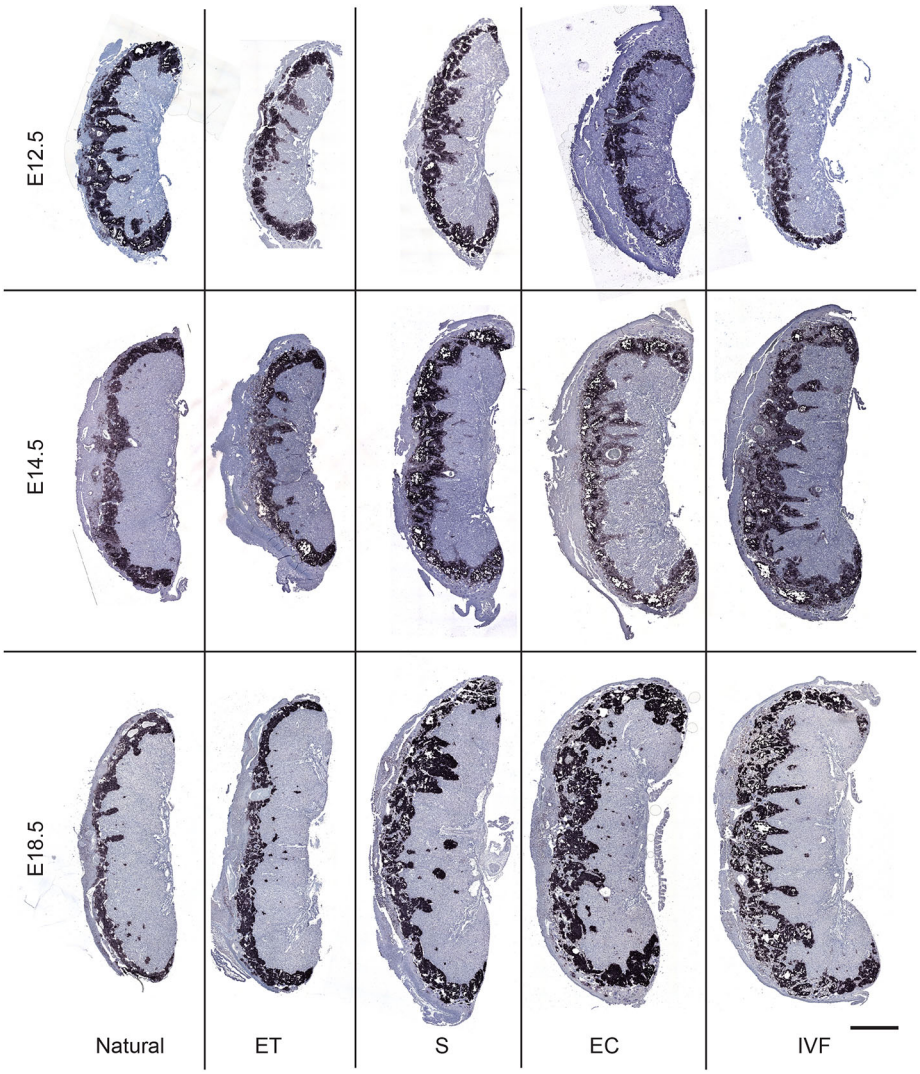


**Fig. 4. Representative mouse placental sections at E12.5, E14.5 and E18.5 using *Tpbpa in situ* hybridization.** *In situ* hybridization was performed on placenta cross-sections using the junctional zone marker *Tpbpa*. Sections were counterstained with Hematoxylin. Scale bar: 1000 µm.

when accounting for the difference in total placental size (Fig. 6A,B). By E18.5, only the EC group had proportionally more P-TGCs than natural placentas (Fig. 6C). Although the majority of the junctional zone comprised spongiotrophoblasts in all groups at all time points (Fig. 6D-F), EC and IVF placentas displayed a disproportionate increase in glycogen cells at E18.5 (Fig. 6F-K). In EC and IVF placentas, 26-30% of the junctional zone comprised glycogen cells compared with only 13% in controls. Because glycogen cells are known to deplete their glycogen stores prior to term (Coan et al., 2006), we determined by Periodic acid-Schiff staining whether glycogen cell content was abnormally retained in IVF placentas in a subset of E18.5 IVF and control placentas. Despite differences in the total amount and proportional contribution of glycogen cells to the junctional zone at E18.5, IVF placental glycogen content relative to glycogen cell area was not significantly different from controls, suggesting that placental glycogen stores were normally used prior to term (Fig. S5).

### IVF increases sFLT1 levels, a protein implicated in causing preeclampsia

Given the known increase in risk of preeclampsia among IVF patients, and the observation of impaired vasculature, enlarged junctional zone and reduced fetal size in EC and IVF groups in our mouse model, we measured expression of the anti-angiogenic factor, soluble Fms-like tyrosine kinase-I (*sFlt1*), which is the soluble, non-membrane associated splice variant of Fms-like tyrosine kinase (*Flt1*). Increased circulating maternal levels of sFLT1 are strongly implicated in the etiology of preeclampsia (Palmer et al., 2016). The link between sFLT1 and ART is less clear – two studies have reported significantly increased sFLT1 in ART pregnancies, whereas two others have reported no differences (Côté et al., 2019; Joy et al., 2015; Lee et al., 2015; Sanchez et al., 2012). In mice, increased *sFlt1* expression or protein, which is normally produced by the junctional zone, induces preeclampsia-like symptoms (Bergmann et al., 2009; Maynard et al., 2003). Compared with natural controls, we observed a significant decrease in *sFlt1* expression in EC and IVF groups at E12.5 (Fig. 7A). At E14.5, there are no significant differences among groups; however, at E18.5, EC and IVF groups had significantly increased *sFlt1* expression compared with natural controls. Notably, the EC group had two individual outliers with extremely high *sFlt1* expression (Fig. S6).

To test whether this late gestational increase in *sFlt1* expression resulted in increased circulating levels of sFLT1 in maternal blood and changes in blood pressure, we assessed a cohort of IVF dams at E18.5. To control for litter size, IVF dams were compared with ET controls, which exhibit *sFlt1* expression and birth weight comparable with naturals. Indeed, controlling for litter size is

Development (2020) 147, dev186551. doi:10.1242/dev.186551

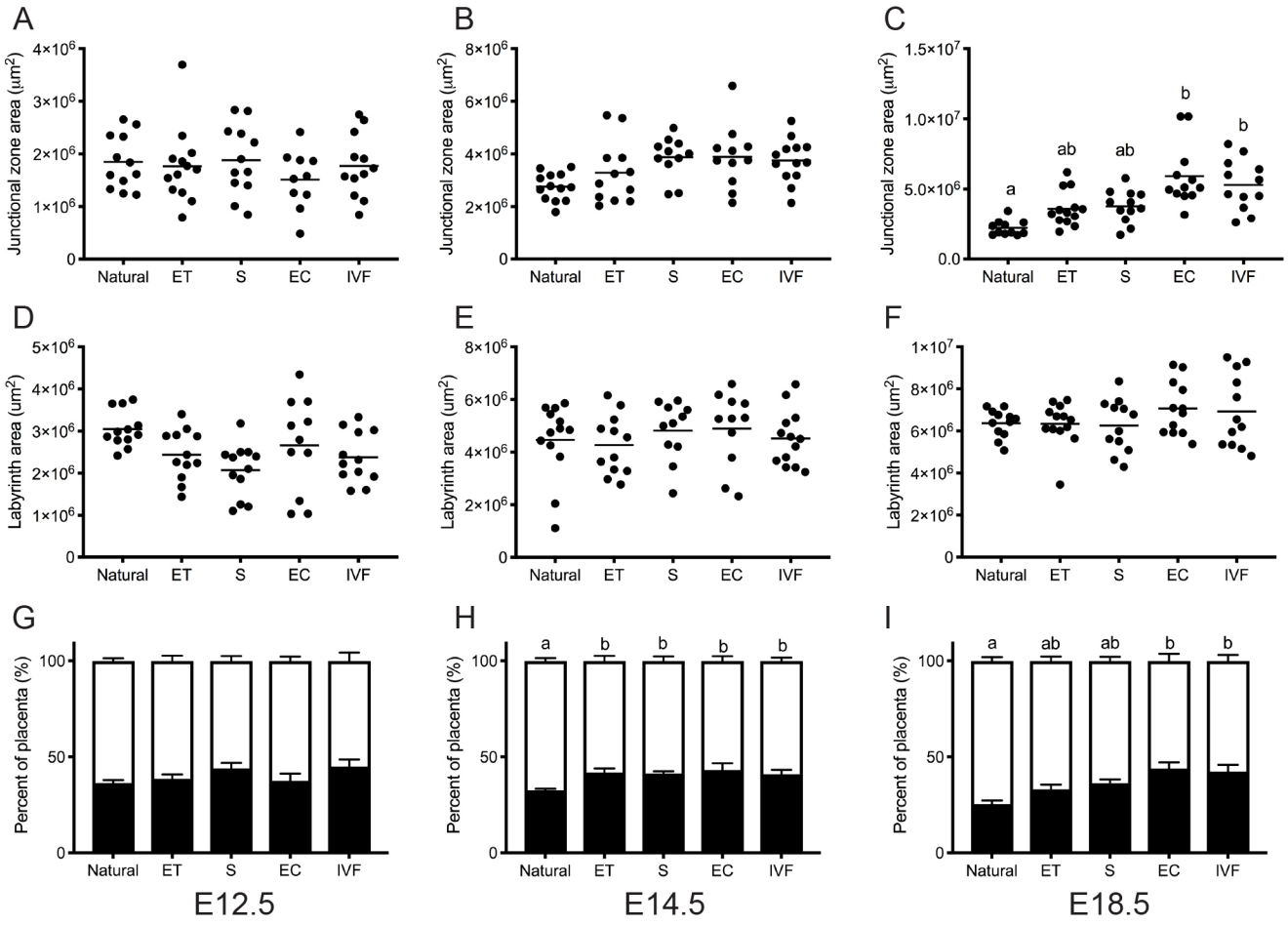


**Fig. 5. Percentage of placental junctional zone in a mouse model of IVF procedures at E12.5, E14.5 and E18.5.** (A-C) Total junctional zone area was measured using *Tpbpa in situ* hybridization probes (*n*=10-13/group). (A) E12.5, (B) E14.5 and (C) E18.5. Black line represents the mean of each group. (D-F) Labyrinth area was measured using *Tpbpa in situ* hybridization probes (*n*=10-13/group). (D) E12.5, (E) E14.5 and (F) E18.5. Black line represents the mean of each group. (G-I) Junctional zone and labyrinth area as a percentage of the total placental area, excluding the decidua and chorionic plate (*n*=10-13/group). Black bar represents junctional zone percentage, white bar represents labyrinth percentage. Data are mean±s.e.m. A significant ($P<0.05$) global likelihood ratio test of differences between groups in the mixed effects model was followed by pairwise tests adjusted using a Holm-Bonferroni correction. Groups with different letters denote significant differences between groups (adjusted $P<0.05$); the same letters indicate no difference was detected. For E14.5 junctional zone/labyrinth ratio, raw *P*-values rather than adjusted *P*-values were used to infer pairwise differences among experimental groups, acknowledging that the use of raw *P*-values does not strictly control the family-wise type I error rate.

important, as our data show that circulating sFLT1 is positively correlated with litter size (Fig. 7D). When normalized by litter size, IVF dams had significantly increased sFLT1 serum levels by comparison with ET controls (Fig. 7D,E). Although circulating sFLT1 was increased in IVF dams, this increase did not result in an observable increase in blood pressure levels (Fig. 7F).

### Significant DNA methylation changes are associated with embryo culture but are stable across placental development

In addition to placenta overgrowth, IVF placentas exhibit biallelic expression of imprinted genes, which are normally monoallelically expressed, concomitant with loss of allele-specific DNA methylation of their regulatory imprinting control regions (ICRs) (de Waal et al., 2014; de Waal et al., 2015; Rahimi et al., 2019; Whidden et al., 2016). To ascertain whether an association exists between these DNA methylation changes and the morphological phenotypes over the span of placenta development, we measured DNA methylation of the paternally methylated ICR *H19/Igf2* and three maternally methylated ICRs – *Kcnq1ot1*, *Peg3* and *Snrpn* – by bisulfite pyrosequencing. These loci were chosen due to their known role in human imprinting disorders and known function in placental and fetal growth (Rhon-Calderon et al., 2019; Tunster et al., 2013, 2018). Because ICRs exhibit methylation on one parental allele, assay of bulk DNA results in ∼50% methylation. For *H19*, *Igf2*, *Kcnq1ot1* and *Peg3*, ICR DNA methylation levels were significantly different between EC and/or IVF groups compared with controls at all time points (Fig. 8A-I). For *Snrpn*, ICR DNA methylation levels were significantly different for the embryo culture group compared with natural controls at E12.5 and E18.5, but not at E14.5 (Fig. 8J-L). ET and S groups were not significantly different from natural controls for all ICRs and time points. Thus, procedures that entail embryo culture were associated with ICR methylation defects. Notably, ICR DNA methylation levels in EC and IVF placentas were not further reduced from E12.5 to E18.5, suggesting that mechanisms maintaining ICR methylation specifically after placenta formation to term were intact.

We have previously shown that term IVF placentas have reduced global DNA methylation levels at repetitive elements using the luminometric methylation assay (LUMA) (de Waal et al., 2015). To assess whether global DNA methylation changes are associated

Development (2020) 147, dev186551. doi:10.1242/dev.186551

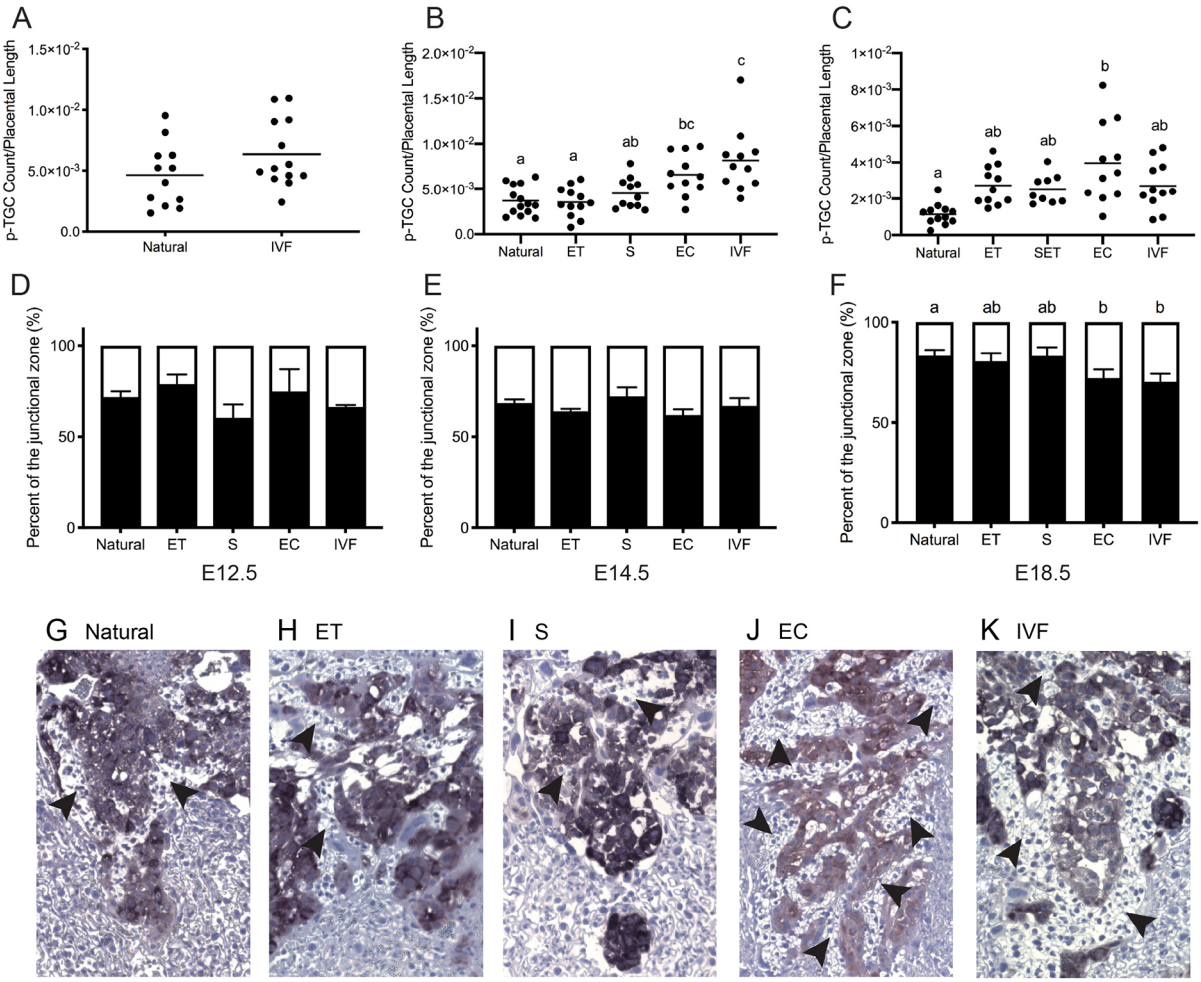


**Fig. 6. Spongiotrophoblast and glycogen cell percentage in a mouse model of IVF procedures at E12.5, E14.5 and E18.5.** (A-C) p-TGCs were counted and normalized by placental length at E12.5, E14.5 and E18.5, respectively. (D-F) Spongiotrophoblast and glycogen cell area were measured using spongiotrophoblast marker, *Prl8a8*, *in situ* hybridization probes and characteristic glycogen cell morphology, respectively. White and black bars represent glycogen cell and spongiotrophoblast area, respectively, as a percentage of the total junctional zone area ($n$=6 per group). A significant ($P$<0.05) global likelihood ratio test of differences between groups in the mixed effects model was followed by pairwise tests adjusted using a Holm-Bonferroni correction. Groups with different letters indicate significant differences between groups ($P$<0.05); the same letters indicate no difference was detected. For E14.5 pTGCs, raw $P$-values rather than adjusted $P$-values were used to infer pairwise differences among experimental groups, acknowledging that the use of raw $P$-values does not strictly control the family-wise type I error rate. (G-K) Representative images of E18.5 placental sections after *Prl8a8 in situ* hybridization from (G) Natural, (H) ET, (I) S, (J) EC and (K) IVF groups. Images captured at 20× magnification. Arrowheads indicate patches of glycogen cells.

with embryo culture similar to ICR DNA methylation changes, we conducted LUMA analysis. We determined that global DNA methylation levels indeed were significantly reduced in EC and IVF groups at all time points compared with controls and S groups (Fig. 8M-O), supporting the proposal that the embryo culture drives placental hypomethylation. The ET group displayed intermediate DNA methylation levels that were not statistically different from controls, EC or IVF groups.

## DISCUSSION

A matter of increasing clinical relevance is why ART pregnancies are at greater risk for certain pregnancy complications. Although performed on a small number of total dams per group to accommodate the multiple time points and experimental groups, to our knowledge, this is the first experimental study to demonstrate that ART procedures independent of factors related to underlying infertility lead to placental vasculature defects and increased sFLT1, cellular phenotypes relevant to preeclampsia in humans. Specifically, our model suggests that factors related to embryo transfer alone confer an initial increased risk of impairment in placental vascularization and fetal growth shortly after placental formation. At this time point, ET, S, EC and IVF placentas are morphologically indistinguishable from each other. By term, transferred embryos that were not exposed to *in vitro* culture show placental vasculature improvement and fetal catch up growth. Embryos that were cultured, however, have compromised fetal growth throughout pregnancy that is associated with late gestational placental overgrowth, increased sFLT1 levels and underlying placental DNA hypomethylation.

### ART procedures interfere with early placental vascularization

A striking and unanticipated finding is that all ART experimental groups, ET, S, EC and IVF, have reduced fetal growth shortly after placenta formation when compared with natural controls. This outcome is different from previous studies, which have predominantly compared IVF concepti to S or ET controls, rather than natural controls. The inclusion of all groups for comparison in

Development (2020) 147, dev186551. doi:10.1242/dev.186551

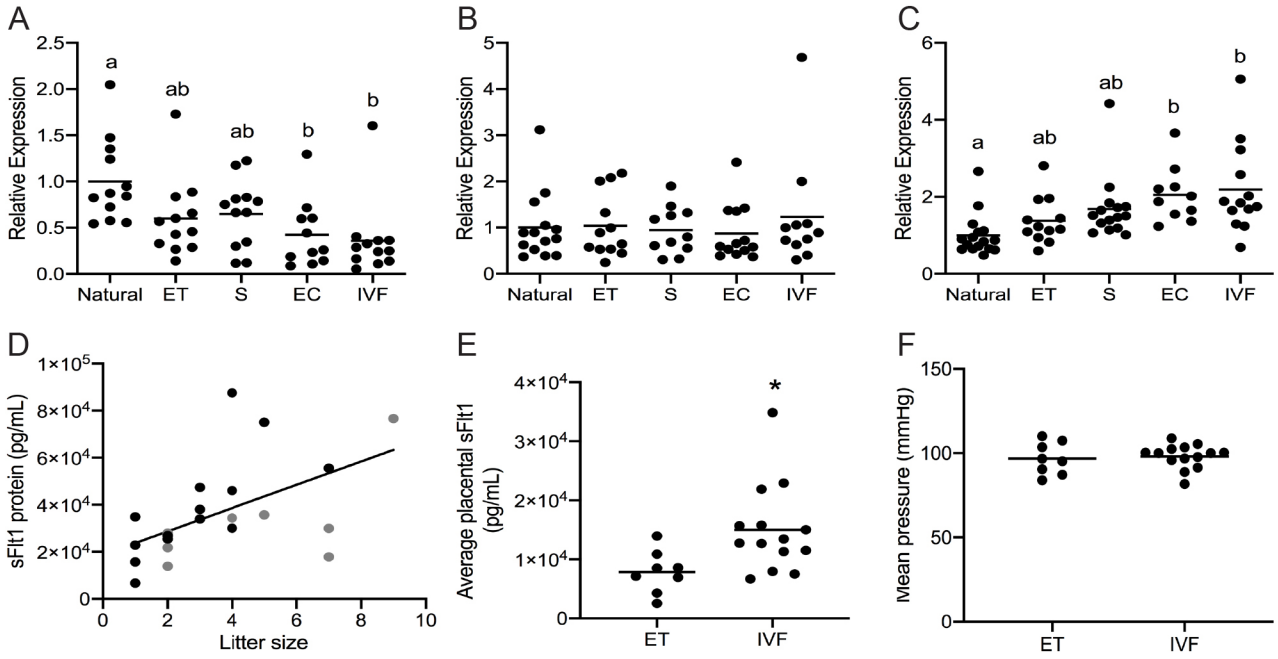


**Fig. 7. Placental *sFlt1* expression, sFLT1 protein levels and maternal blood pressure in a mouse model of IVF procedures.** (A-C) Placental *sFlt1* levels at (A) E12.5, (B) E14.5 and (C) E18.5. Each data point represents an individual placenta from a minimum of three different litters ($n$=10-13 per group). A significant ($P$<0.05) global likelihood ratio test of differences between groups in the mixed effects model was followed by pairwise tests adjusted using a Holm-Bonferroni correction. Groups with different letters indicate significant differences between groups (adjusted $P$<0.05); the same letters indicate no difference was detected. (D) Maternal sFLT1 protein concentration in maternal serum according to litter size. Each data point represents a single dam at E18.5 of pregnancy: ET (gray) and IVF (black). Line represents best-fit value ($P$=0.010). (E) Average placental contribution to sFLT1 at E18.5. Statistical significance was determined by Student's $t$-test (*$P$<0.05). (F) Maternal mean arterial blood pressure in ET and IVF dams at E18.5 ($P$>0.05).

this study aids in determining how ET and S still contribute some effects among the various phenotypes. However, there is a caveat to the comparison with natural concepti because of the inability to control both the timing of implantation and overall litter size, with an attendant impact on fetal weight and placentation results. Our histological and molecular analyses of labyrinth cells suggest that factors related to embryo transfer can lead to a generalized defect in labyrinth development at mid-gestation; such defects would presumably impair gas and nutrient exchange (Woods et al., 2018). This outcome differs from a recent study that compared E10.5 ET and natural concepti (Menelaou et al., 2020). This study reported significantly smaller ET placentas compared with naturals, with no differences in fetal weight. Together with E10.5 placental transcriptomic analysis, the authors concluded that embryo transfer significantly impacts placental transcriptome and growth, with signs toward adaptive responses that would improve placental function. This supports our observation that fetal weights early in gestation are unaffected by factors related to embryo transfer. We postulate that, by E12.5, as fetal growth increases, fetal weight differences may become more apparent, noting that we cannot discount differences in mouse strain and embryo transfer procedures to explain the discrepancy between the studies. The overall conclusion that ET placentas mount an adaptive response (Menelaou et al., 2020) aligns with our results. We find no statistical difference in fetal blood vessel density or syncytiotrophoblast cell marker gene expression at later time points, indicating some vasculature improvement in all ART groups. However, the cell marker for sinusoidal trophoblast giant cells, *Ctsq*, remains reduced in the IVF group. A study performed by Outhwaite et al. demonstrates the importance of sinusoidal trophoblast giant cells in late gestation. Ablation of 80% of the cells results in drastically impaired fetal growth late in gestation and embryonic lethality, without impacting placental weight (Outhwaite et al., 2015). From this result, the authors concluded that sinusoidal trophoblast giant cells likely maintain labyrinth structure and that the hormones they secrete are important for fetal growth. In our study, the ET and S group show fetal growth catch up, demonstrating that early impairment in vascularization and a smaller starting fetal weight can be overcome. In contrast, the EC and IVF groups do not reach fetal weights comparable with natural controls at E18.5. This finding strongly suggests that embryo culture procedures interfere with fetal weight catch up mechanisms, possibly through permanent alteration to sinusoidal trophoblast giant cells.

A question that emerges from our findings is whether ARTs predispose embryos to early impairments in vascularization in humans. Although there is sufficient evidence that ART procedures contribute to increased risk for both small- and large-for-gestational age offspring at birth, there is conflicting information regarding fetal growth and placentation in IVF pregnancies earlier in gestation. Most assessments are limited to crown-rump length measurements, estimates of fetal and placental volume, and uterine artery pulsatility index, a measure of uteroplacental perfusion. Two groups found that first trimester placental volume is significantly reduced in fresh IVF cycles compared with natural conceptions (Choux et al., 2019; Rizzo et al., 2016). Another group found that a specific embryo culture medium is associated with lower birth weight and that fetal weight differences could be detected as early as the second trimester (Dumoulin et al., 2010; Nelissen et al., 2012; Nelissen et al., 2013). Many studies, however, did not find any differences in first and/or second trimester fetal growth and none have identified any differences in uteroplacental perfusion (Carbone et al., 2011; Conway et al., 2011; Eindhoven et al., 2014; Sundheimer et al.,

Development (2020) 147, dev186551. doi:10.1242/dev.186551

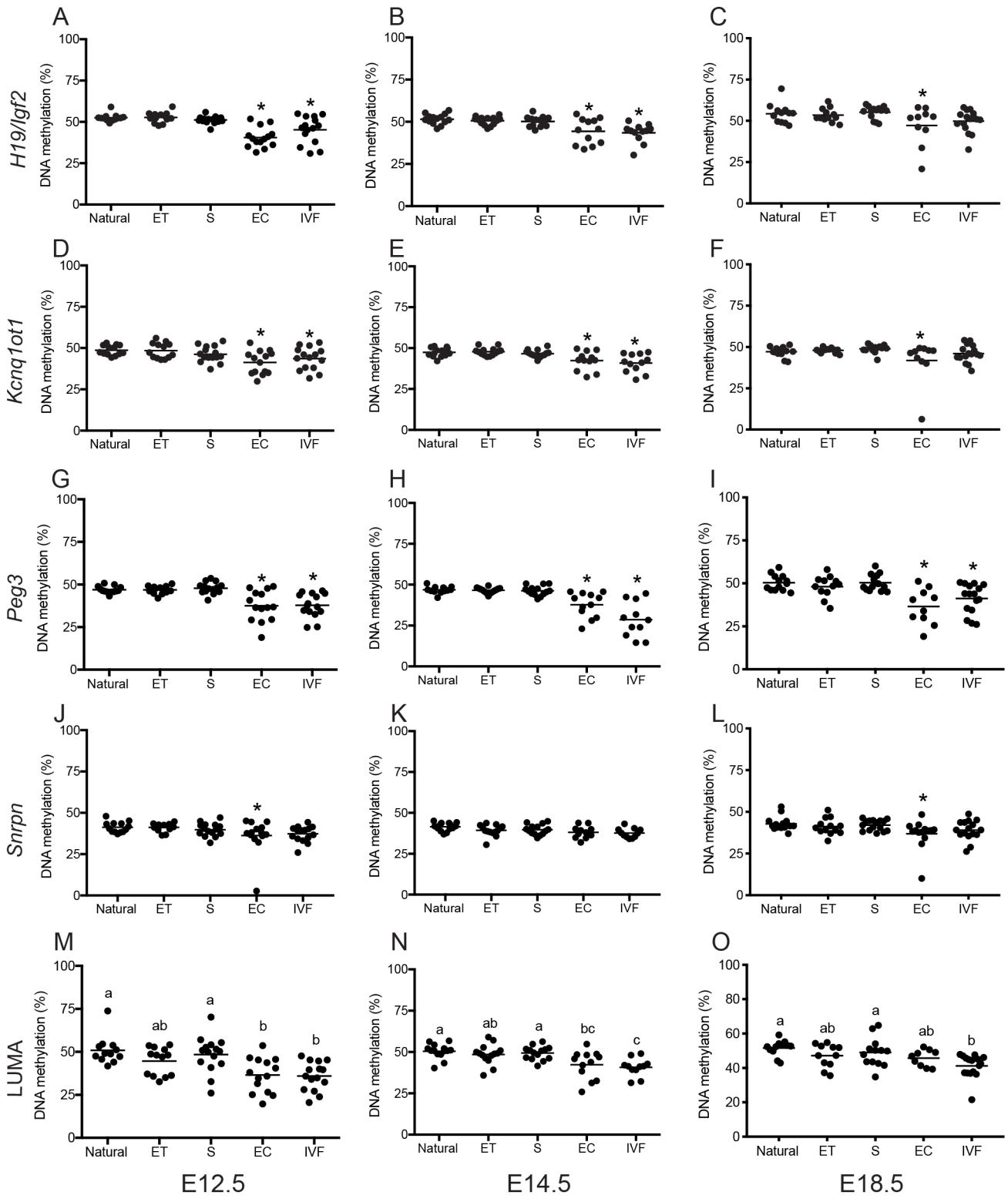


**Fig. 8. DNA methylation status in E12.5, E14.5 and E18.5 placentas after IVF procedures.** (A-O) Each data point represents an individual placenta from a minimum of three different litters ($n$=10-13 per group). Statistical significance of imprinted gene assays was determined for each end point using the $F$-ratio test. Groups with asterisks are significantly different from groups with no asterisks (*$P$<0.05). A significant (*$P$<0.05) global likelihood ratio test of differences between groups in the mixed effects model was followed by pairwise tests adjusted using a Holm-Bonferroni correction. Groups with different letters indicate significant differences between groups (adjusted $P$<0.05); the same letters indicate no difference was detected.

2018). As live imaging technologies improve, so will the ability to detect early differences in fetal and placental growth. The labyrinth defects in our study, however, were observed only at the histological and molecular levels. Because no differences in placental weight are detected until later in development, live imaging of placental volume may not be sufficient to detect subtler vasculature

Development (2020) 147, dev186551. doi:10.1242/dev.186551

impairment, supporting the need for more sensitive non-invasive technologies.

### ART procedures, independent of infertility, induce cellular behavior in late gestation reflective of human placental pathologies associated with ART

As noted in previous studies, the late gestational placenta overgrowth phenotype in mouse is relevant to human IVF placentas that also display overgrowth and increased thickness (Choux et al., 2019; Daniel et al., 1999; Haavaldsen et al., 2012; Joy et al., 2012; Zhang et al., 2011). Here, we demonstrate that embryo culture from the 1-cell to blastocyst stage results in the most dramatic increases in placental weight and differences in junctional zone cell composition, suggesting that the embryo culture procedure is the largest driver of placental overgrowth observed in humans.

Although the molecular mechanisms that lead to morbidly adherent placentation in humans remain unclear, there is evidence that evasion of growth suppression, activation of invasion, sustained proliferation, resistance to cell death, local pro-angiogenic environment, reprogramming of energy metabolism and evading immune destruction need to occur (Bartels et al., 2018). Notably, a number of these hallmarks are evident in EC/IVF mouse placentas that exhibit continuous growth from E14.5 to E18.5, a time when placenta growth normally ceases and junctional zone cells show invasive finger-like projections into the labyrinth. Both phenotypes suggest evasion of growth suppression and activation of invasion. Indeed, sustained proliferation in IVF placentas when compared with ET controls has already been demonstrated by Bloise et al. (Bloise et al., 2012). Furthermore, loss of the defined border between junctional zone and labyrinth tissues in EC/IVF placentas suggests disruption of cellular signals that keep the tissue layers distinct from one another. Retention of glycogen cells in EC/IVF mouse placentas at E18.5, a time after glycogen cells are known to normally undergo apoptosis (Bouillot et al., 2006), suggests cell death resistance. EC/IVF placentas also display improved fetal blood vessel density at time points coinciding with junctional zone overgrowth/invasion into the labyrinth, suggesting a local pro-angiogenic environment within the labyrinth is present.

Our analysis of *sFlt1* provides new insight into the increased risk of preeclampsia with ARTs. We observed a modest, but significant increase in *sFlt1* expression in EC and IVF placentas, and identified two concepti with abnormally high *sFlt1*. Our analysis of serum sFLT1 levels indeed supports the observation that IVF placentas produce significantly more sFLT1 protein and there is marked variability among dams in the IVF group when compared with the ET group. Increased sFLT1 in IVF pregnancies has been noted in clinical studies (Lee et al., 2015; Sanchez et al., 2012). Importantly, our study suggests that some of that sFLT1 increase is independent of underlying infertility factors and can be specifically attributed to embryo culture. Although there is a well-established link between IVF and preeclampsia in humans, to date, very few clinical studies have assessed circulating sFLT1 levels in IVF pregnancies and none has assessed *sFlt1* expression or protein levels in the placenta. In the rodent model, there is more variability in sFLT1 levels among IVF individuals than the ET control group, suggesting a stochastic response to IVF procedures. Indeed, an increase in variability is observed in many of the morphological and epigenetic end points we assessed. Understanding the mechanisms underlying this stochasticity may explain why preeclampsia occurs with some IVF pregnancies but not others. Although we do not observe a significant increase in blood pressure, we believe this to be a limitation of the mouse model. Owing to use of non-surgical embryo transfer, ET and IVF mouse pregnancies have anywhere between 31 and 92% fewer pups than those expected for natural pregnancies. Thus, circulating sFLT1 levels are under the threshold levels needed to result in preeclampsia-like increased blood pressure in dams. We do not discount the possibility that other factors related to infertility or maternal predisposition may play a considerable role in preeclampsia development in humans. Currently, it is unclear why *sFlt1* expression is significantly lower in E12.5 EC and IVF placentas compared with controls, as there are no obvious differences in placenta weight or proportion of junctional zones where *sFlt1* is expressed. Nonetheless, these findings suggest that there can be a dynamic change of factor expression over the course of placental development. Thus, in future studies, it will be important to determine the role of sFLT1 and other anti-angiogenic/angiogenic factors not only in late gestation ART pregnancies, but also at earlier developmental time points.

### Embryo culture causes placental epigenetic changes concomitant with the most dramatic term outcomes

Our study demonstrates that embryo culture causes the most dramatic fetal and placental outcomes by term. Importantly, our assessment of both global levels of DNA methylation and at imprinting control regions support the observation that, although placental DNA methylation is reduced by the embryo culture procedure, it is stable throughout placenta development. Previous studies have shown that DNA methylation loss during embryo culture is already detectable at the blastocyst stage in both mice and humans (Doherty et al., 2000; Fauque et al., 2007; Mann et al., 2004; White et al., 2015). Our results support the hypothesis that loss of DNA methylation occurs specifically during the embryo culture period through failure to maintain DNA methylation during preimplantation embryo development. However, once embryos are transferred to the uterine environment and the placenta is formed, DNA methylation levels are faithfully maintained and there is no further loss. How embryo culture results in loss of DNA methylation is poorly understood. Rabbit embryos cultured in two different media exhibited a reduction in *Tet1* and *Tet2* expression, genes that encode enzymes involved in active demethylation. No differences in *Dnmt1*, *Dnmt3a* or *Dnmt3b* genes, coding for enzymes involved in maintenance and *de novo* DNA methylation, were detected (Salvaing et al., 2016). A study using human embryos observed abnormalities in DNMT3B levels and localization in poorer quality embryos compared with high-quality embryos (Petrussa et al., 2014). Because all human embryo data come from individuals undergoing some form of ART, these studies lack a non-ART control group, making it impossible to assess the full extent of ART effects. With regards to the placental phenotype, several imprinted gene knockout or overexpression mouse models provide a clear link between the loss of imprinted gene regulation and placental phenotypes similar our ART model (John, 2013). Whether and how epigenetic differences resulting from embryo culture directly drive these robust replicable phenotypes in the late gestation placenta remains to be determined.

The morphological and epigenetic changes that occur in mouse placenta in response to ART procedures are robust. Why otherwise normal term IVF pregnancies in humans do not display such pronounced phenotypes is unclear, but the differences are likely due to several factors, including reduced genetic variation, short duration of gestation, and controlling for age, fertility and environmental conditions in the mouse model. Furthermore, human studies are often confounded by supra-physiological hormonal levels in the recipient, which in both human and mouse

Development (2020) 147, dev186551. doi:10.1242/dev.186551

studies induce a smaller placenta phenotype (e.g. Mainigi et al., 2013; Rizzo et al., 2016). This cumulative effect could mask placental abnormalities in humans.

The mouse ART model provides an excellent opportunity to interrogate how ART procedures result in placental defects and the compensatory mechanisms that exist to facilitate fetal growth under insult. Our results indicate that ART procedures can induce placental vasculature defects, overgrowth and increased sFLT1 levels – cellular phenotypes that are clinically relevant to placental abnormalities observed with ART in humans. Our study also suggests that embryo culture causes the most severe placental phenotypes among the individual IVF procedures and is associated with reduced fetal growth. Thus, future research to improve embryo culture may ameliorate adverse outcomes due to abnormal placentation in humans.

## MATERIALS AND METHODS

### Animals

Breeding stocks of CF1 female mice (Envigo, Wilmington, MA, USA), B6SJLF1 (The Jackson Laboratory), and CD-1 (Charles River, Indianapolis, IN) male mice were maintained in a pathogen-free facility. All animals were housed in polysulfone cages containing drinking water and chow (Laboratory Autoclavable Rodent Diet 5010, LabDiet) *ad libitum*. All animal work was conducted with the approval of the Institutional Animal Care and Use Committee and the University of Pennsylvania.

### Generation of natural, ET, S, EC and IVF concepti

All CF-1 female mice were sexually mature and used between 2 and 3 months of age. Naturally conceived concepti were generated by mating naturally cycling CF1 females to B6SJLF1 males. The day a vaginal plug was detected was denoted as embryonic day (E) 0.5 and development occurred *in vivo* without blastocyst transfer. ET concepti were generated by mating naturally cycling females to B6SJLF1 males and blastocysts were flushed from both uterine horns on E3.5 using warm HEPES-buffered minimum essential media (MEM) and immediately transferred to a CF1 2.5 day pseudopregnant recipient using non-surgical embryo transfer (NSET) devices (Paratechs). S concepti were generated by superovulating CF1 females using standard gonadotropin protocols and mating them to B6SJLF1 males (Behringer et al., 2014a). Blastocysts were flushed and transferred as performed for the ET group. EC concepti were generated by superovulating and mating CF1 females identical to the S group. One-cell embryos were flushed from the oviducts using MEM and cultured in EmbryoMax KSOM medium (1×) containing ½ Amino Acids (KSOM+AA, EMD Millipore) in an incubator under optimized conditions (37°C, 5% $CO_2$, 5% $O_2$, 90% $N_2$) (Behringer et al., 2014b). Blastocysts were transferred from the KSOM+AA culture droplet and washed through four droplets of MEM for a few seconds prior to transfer. IVF concepti were generated according to optimized protocols recommended by the Jackson Laboratory (Behringer et al., 2014c). Briefly, eggs from superovulated CF1 females were fertilized in EmbryoMax Human Tubal Fluid (1×) media (HTF, EMD Millipore) using capacitated B6SJLF1 sperm collected from the cauda epididymides and vas deferens. After 4 h, eggs were washed in HTF media and KSOM+AA media before culturing in KSOM+AA. Blastocysts were transferred from the culture droplet and briefly washed in MEM prior to transfer. Pseudopregnant recipients (2.5 days post-copulation) were generated by mating CF1 females with CD-1 vasectomized males. Use of 2.5 dpc pseudopregnant females is considered optimal over 3.5 dpc because manipulated embryos have time to catch up developmentally (Nagy et al., 2003). Each pseudopregnant recipient received ten ET, S, EC or IVF blastocysts. Day of blastocyst transfer was defined as E3.5 and concepti were collected at E12.5, 14.5 and 18.5 (+9.0, 11.0 and 15.0 days after transfer, respectively). All groups were generated concurrently and CF1 females were randomly assigned as a natural, ET, S, EC, IVF or pseudopregnant recipient. Males were randomly assigned as male sire or IVF sperm donor. The same male sires used to generate natural concepti were used to generate ET, S and EC concepti.

### Tissue collection

Concepti were collected at E12.5, E14.5 or E18.5. Naturally mated females or pseudopregnant recipients were euthanized and fetuses and placentas were dissected. Fetal and placental wet weights were recorded (Fig. 1, Figs S2 and S4). Fetal tissue was snap frozen in liquid nitrogen and used for sex genotyping. Placentas were cut in half through the umbilical cord attachment site. Half of the placenta was snap frozen in liquid nitrogen and stored at −80°C for DNA and RNA isolation. The other half of the placenta was fixed in 10% phosphate-buffered formalin. Fixed tissues were then processed through an ethanol dehydration series and xylenes prior to embedding in paraffin wax. Tissue sections (5 µm) were prepared for histological analyses. A minimum of 11 concepti per experimental group per timepoint from a minimum of three different dams were analyzed for all histological and molecular assays, with representation from all litters. Eleven concepti per group provides the power to detect significant differences in fetal weight, placental weight and loss of imprinting based on our previous observations, with an $\alpha$=0.05. In litters of two or more concepti, one female and one male were selected for analysis if possible. After considering sex, concepti with values closest to the litter mean for placental weight were selected to avoid potential selection bias for litters of three or more concepti.

### Sex genotyping

Sex was determined by reverse transcriptase PCR using primers for *Kdm5c* and *Kdm5d* using genomic DNA isolated from fetal tissue of each conceptus as previously described (SanMiguel et al., 2018).

### *In situ* hybridization

Antisense and sense control *in situ* hybridization probes were designed, synthesized and hybridized as previously described (Bany and Simmons, 2014) (probe information is detailed in Table S4). Antisense *in situ* hybridization probe was thermally denatured at 65°C for 5 min and applied to tissue sections (100 µg probe in 75 µl of hybridization buffer per section), while sense *in situ* hybridization probe control was added to a negative control slide. Sections were covered with glass coverslips, sealed with rubber cement and incubated overnight at 65°C in humid chambers. Anti-DIG-AP Fab fragments (Sigma-Aldrich) (1:1000) were applied to sections for 1 h at room temperature. Slides were counterstained with Harris Hematoxylin and mounted using ImmunoHistoMount (Sigma-Aldrich). Slides were imaged using an EVOS FL Auto Cell Imaging System and software (Life Technologies) at 20× magnification. The junctional zone (*Tpbpa*-positive), spongiotrophoblasts (*Prl8a8*-positive), glycogen cells (junctional zone *Prl8a8*-negative cells with glycogen cell morphology) and whole placenta area, excluding residual decidua, were measured using FIJI (ImageJ v2.0.0, National Institutes of Health) or Adobe Photoshop by measurers blinded to the experimental group. The percentage of junctional zone present was calculated as the total junctional zone area/whole placenta area (excluding decidua) ×100. Percentage of spongiotrophoblasts present in the junctional zone was calculated as the total spongiotrophoblast area/junctional zone area ×100. The percentage of glycogen cells was calculated as the total glycogen cell area/junctional zone area ×100.

### Immunostaining

Placental sections were passed through xylenes, followed by a graded ethanol rehydration series and phosphate-buffered saline (PBS). Antigen retrieval was performed by pressure cooking slides submerged in Antigen Unmasking Solution (Vector Laboratories) for 20 min. Sections were washed in tap water and quenched with 30% hydrogen peroxide/methanol solution. Sections were washed in PBS and 15% normal goat serum was applied to tissue sections for 1 h at room temperature. CD34 primary antibody (Abcam, ab81289) was applied to tissue sections at a dilution of 1:400 for 1 h at room temperature, then overnight at 4°C. For negative control slides, 15% normal goat serum was re-applied without CD34 primary antibody. The next day, slides were washed with PBS, secondary goat anti-rabbit antibody (Vector Laboratories) was applied to all slides at 1:1000 for 1 h and the Ready-to-use Vectastain Universal ABC kit and Vector NovaRED Peroxidase (HRP) Substrate Kits were used according to manufacturer's instructions (Vector Laboratories). Robust positive staining

Development (2020) 147, dev186551. doi:10.1242/dev.186551

was observed in fetal endothelial cells of the labyrinth, as previously reported (Parchem et al., 2018). Slides were counterstained with Harris Hematoxylin, dehydrated in a graded ethanol series and xylenes, and mounted with glass coverslips using Permount mounting medium. Slides were imaged using an EVOS FL Auto Cell Imaging System and software (Life Technologies) at 20× magnification. Labyrinth area and whole placenta area excluding decidua were measured using FIJI (ImageJ v2.0.0, National Institutes of Health) or Adobe Photoshop by measurers blinded to experimental group. Labyrinth area was calculated as the total junctional zone area/whole placenta area (excluding decidua) ×100.

### Fetal endothelial cell histological analyses

Placental sections stained with CD34 primary antibody were scanned and digitized using the Aperio Scanscope CS-O slide scanner at the Children's Hospital of Philadelphia Pathology Core Laboratory. Aperio Imagescope software was used to outline the labyrinth area and the Aperio Microvessel Analysis algorithm was performed. Area was traced by individuals blinded to experimental group. Algorithm macros were optimized for the algorithm to accurately detect CD34-positive vessels using manufacturer's guidelines. Data are the algorithm-measured areas of CD34-positive staining relative to labyrinth area. Individual data points are the average of two separate placental sections: one section taken from within the first 50 µm from the center of the placenta, and the other section taken >50 µm from the first analyzed section.

### Periodic acid-Schiff staining

Periodic acid-Schiff (PAS) staining was performed using a PAS staining kit according to manufacturer's guidelines (EMD Millipore). Briefly, placental sections were passed through xylenes, followed by a graded ethanol rehydration series and distilled water. Slides were passed through periodic acid solution for 5 min, sulfite water three times for 2 min each, tap water for 3 min and rinsed in distilled water, then passed through Schiff's reagent for 15 min, tap water for 3 min and rinsed in distilled water. Slides were counterstained with Gill II Hematoxylin, rinsed in tap water, dehydrated in a graded ethanol series and xylenes, and mounted with glass coverslips using Permount mounting medium. Slides were scanned and digitized using the Aperio Scanscope CS-O slide scanner at the Children's Hospital of Philadelphia Pathology Core Laboratory. Aperio Imagescope software was used to outline intact glycogen cell area and the Aperio Color Deconvolution Analysis algorithm was performed. Areas were traced by individuals blinded to experimental group. Algorithm macros were optimized for the algorithm to accurately detect PAS-positive staining using manufacturer's guidelines. Data are the average intensity of PAS-positive staining relative to glycogen cell area. Individual data points are the average of all glycogen cells from two separate placental sections: one section taken from within the first 50 µm of the center of the placenta; the other section taken more than 50 µm from the first analyzed section.

### DNA and RNA isolation

DNA and RNA were simultaneously isolated from one-quarter of each snap-frozen placenta as previously described (de Waal et al., 2014).

### Quantitative qPCR for labyrinth cell markers

cDNA was synthesized from isolated RNA as previously described (de Waal et al., 2014). Real-Time quantitative PCR was performed using QuantStudio 7 Flex Real-Time PCR System (Life Technologies) using the Power SYBR Green master mix (Applied Biosystems) with 0.37 µM primer concentrations. For each primer set (primer information is detailed in Table S5), the reaction efficiency (E) was estimated using a standard curve and expression levels were quantified by measuring the cycle threshold (Ct) for each sample using the $E(^{-Ct})$ method. All samples were run in triplicate and performed by individuals blinded to experimental group. Relative expression was calculated using the quantified expression from the endogenous control, *B2m*, which was chosen because of its stable expression level in mouse placenta across multiple samples and experimental groups.

### Blood pressure analyses

Blood pressure analyses were performed by the Mouse Cardiovascular Physiology Core at the University of Pennsylvania. Briefly, invasive blood pressure measurements were performed on E18.5 pregnant dams under isoflurane (1-4%) anesthesia. Mean arterial pressure was measured by inserting Millar catheter probe (SPR-1000) into the carotid artery. Measurements were taken using a Millar MPVS ULTA and ADInstruments LabChart for ∼5 min after catheter insertion. Animals are euthanized by exsanguination and bilateral pneumothorax immediately after blood pressure measurements, and blood and urine samples were collected. Data were analyzed by Core technicians blinded to experimental group of each mouse. A consistent section of aortic pressure was selected and analyzed using the ADInstruments LabChart program.

### sFLT1 enzyme-linked immunosorbent assay (ELISA)

Serum was isolated and stored at −20°C following blood collection after euthanasia. Serum was diluted 1:25 and ELISA was performed in duplicate by individuals blinded to experimental group using Mouse sVEGFR1/FLT1 DuoSet ELISA and DuoSet ELISA Ancillary Reagent Kit 2 (DY471, DY008, R&D Systems) according to manufacturer's instructions.

### Bisulfite pyrosequencing assay

DNA methylation at *H19*, *Igf2*, *Kcnq1ot1*, *Peg3* and *Snrpn* ICRs was measured using bisulfite pyrosequencing of bisulfite-treated DNA as previously described (de Waal et al., 2014) and performed by individuals blinded to experimental group.

### Luminometric methylation assay

Global DNA methylation at repetitive elements was measured using luminometric methylation assays of bisulfite-treated DNA as previously described (de Waal et al., 2014) and performed by individuals blinded to experimental group.

### Statistical analyses

For fetal weight, placental weight, fetal placental ratio, all histological analyses and gene expression outcomes, as well as luminometric methylation assays, we fit a mixed effects model to the data, including ART procedure group as the fixed effect and dam as the random effect. The model was refit without ART procedure group, and a likelihood ratio test used to 'globally' assess evidence for differences in means among the ART procedure groups. If the global test yielded a *P*-value less than the type I error rate of 0.05, we then used pairwise contrasts of the model coefficients to identify pairs of groups with different means. The pairwise tests were adjusted for multiplicity using a Holm-Bonferroni correction in order to strictly maintain the family-wise type I error rate at 0.05. With five groups and ten possible pair-wise comparisons, some outcomes demonstrated evidence of an effect using the global test, but no pairwise contrasts yielded significance for the adjusted *P*-values. We considered the possibility that this discordance reflected reduced power in the pairwise comparisons due to the strict adjustment for multiplicity. In these cases, we used the unadjusted *P*-values to infer differences among groups, acknowledging that this method does not strictly control the family-wise error rate. The approach used is noted in each figure legend. Mixed effects models were fitted using package(nlme) in R v 3.6.2 (R foundation for Statistical Computing; www.R-project.org/). Differences in serum sFLT1 levels and mean arterial blood pressure between ET and IVF dams were assessed using Student's *t*-test. Because previous studies have shown that only a subset of samples exhibit differences at specific imprinted loci (de Waal et al., 2012), variance ratio tests were used to determine evidence that the variance in DNA methylation from bisulfite pyrosequencing assays differed among groups. *t*-tests and variance ratio tests were performed using GraphPad Prism version 8.2.1 and groups were noted as statistically significant if $P<0.05$.

#### Acknowledgements

We acknowledge Jessica Chotiner, Lexie Kaiser, Devin Kenny, Zarrin Subha and Kashviya Suri for their assistance with histological analyses and/or epigenetic analyses. We thank Paula Stein, Teri Ord, Monica Mainigi and Christos Coutifaris for

their technical advice with IVF procedures and helpful comments; Chris Krapp and Joanne Thorvaldsen for their technical expertise with molecular protocols and pyrosequencing; Doris Stoffers for use of the microtome; and Roberto Bonasio for use of the qPCR machine. We thank Malcolm Eaton from the Cross Lab at the University of Calgary for mouse trophoblast *in situ* probes. We acknowledge the CHOP Pathology Core Laboratory for use of embedding equipment and slide scanner services; the Penn Cell and Developmental Biology Microscopy core for use of the imaging facilities; and the Penn Mouse Cardiovascular Physiology Core for performing blood pressure assays.

### Competing interests
The authors declare no competing or financial interests.

### Author contributions
Conceptualization: L.A.V., R.M.S., M.S.B.; Methodology: L.A.V., M.E.P., R.M.S., M.S.B.; Validation: L.A.V., E.A.R.-C., O.Y.C., D.K.N., L.N., A.K.D.; Formal analysis: L.A.V., E.A.R.-C., O.Y.C., D.K.N., L.N., A.K.D., M.E.P.; Investigation: L.A.V., E.A.R.-C., O.Y.C., D.K.N., L.N., A.K.D.; Resources: M.E.P., R.M.S., M.S.B.; Writing - original draft: L.A.V.; Writing - review & editing: L.A.V., E.A.R.-C., O.Y.C., D.K.N., L.N., A.K.D., M.E.P., R.M.S., M.S.B.; Visualization: L.A.V.; Supervision: L.A.V., M.E.P., R.M.S., M.S.B.; Project administration: L.A.V., M.S.B.; Funding acquisition: L.A.V., M.S.B.

### Funding
This work was funded by the National Centers for Translational Research in Reproduction and Infertility (HD068157 to M.S.B.), by a Lalor Foundation Postdoctoral Fellowship (to L.A.V.), by a Ruth L. Kirshstein National Service Award Individual Postdoctoral Fellowship (HD089623 to L.A.V.), by the Roy & Diana Vagelos Scholars Program (O.Y.C. and A.K.D.) and by the National Institute of Nursing Research/National Institutes of Health (T32NR007100 to L.N.). Deposited in PMC for release after 12 months.

### Supplementary information
Supplementary information available online at
http://dev.biologists.org/lookup/doi/10.1242/dev.186551.supplemental

### Peer review history
The peer review history is available online at
https://dev.biologists.org/lookup/doi/10.1242/dev.186551.reviewer-comments.pdf

### References
**Adamson, D. G., Zegers-Hochschild, F., Ishihara, O., Sullivan, E. A., Mansour, R., Nygren, K. G., Banker, M., Dyer, S. and De Mouzon, J.** (2012). ICMART World Report: Preliminary 2008 Data. London, UK.

**Bany, B. M. and Simmons, D. G.** (2014). *50 – Nonradioactive In Situ Hybridization: Optimization for Tissue Sections from Pregnant Uteri and Placenta during the First Half of Pregnancy*. Elsevier.

**Bartels, H. C., Postle, J. D., Downey, P. and Brennan, D. J.** (2018). Placenta accreta spectrum: a review of pathology, molecular biology, and biomarkers. *Dis. Markers* **2018**, 1507674. doi:10.1155/2018/1507674

**Behringer, R., Gertsenstein, M., Nagy, K. V. and Nagy, A.** (2014a). Mouse colony setup. In *Manipulating the Mouse Embryo: A Laboratory Manual*, pp. 92-97. Cold Spring Harbor, NY: Cold Spring Harbor Laboratory Press.

**Behringer, R., Gertsenstein, M., Nagy, K. V. and Nagy, A.** (2014b). Recovery and in vitro culture of preimplantation embryos. In *Manipulating the Mouse Embryo: A Laboratory Manual*, pp. 109-148. Cold Spring Harbor, NY: Cold Spring Harbor Laboratory Press.

**Behringer, R., Gertsenstein, M., Nagy, K. V. and Nagy, A.** (2014c). Assisted Reproduction. In *Manipulating the Mouse Embryo: A Laboratory Manual*, pp. 604-608. Cold Spring Harbor, NY: Cold Spring Harbor Laboratory Press.

**Bergmann, A., Ahmad, S., Cudmore, M., Gruber, A. D., Wittschen, P., Lindenmaier, W., Christofori, G., Gross, V., Gonzalves, A. C. D. C., Gröne, H.-J. et al.** (2009). Reduction of circulating soluble Flt-1 alleviates preeclampsia-like symptoms in a mouse model. *J. Cell. Mol. Med.* **14**, 1857-1867. doi:10.1111/j.1582-4934.2009.00820.x

**Bloise, E., Lin, W., Liu, X., Simbulan, R., Kolahi, K. S., Petraglia, F., Maltepe, E., Donjacour, A. and Rinaudo, P.** (2012). Impaired placental nutrient transport in mice generated by in vitro fertilization. *Endocrinology* **153**, 3457-3467. doi:10.1210/en.2011-1921

**Bloise, E., Feuer, S. K. and Rinaudo, P. F.** (2014). Comparative intrauterine development and placental function of ART concepti: implications for human reproductive medicine and animal breeding. *Hum. Reprod. Update* **20**, 822-839. doi:10.1093/humupd/dmu032

**Bouillot, S., Rampon, C., Tillet, E. and Huber, P.** (2006). Tracing the glycogen cells with protocadherin 12 during mouse placenta development. *Placenta* **27**, 882-888. doi:10.1016/j.placenta.2005.09.009

**Carbone, I. F., Cruz, J. J., Sarquis, R., Akolekar, R. and Nicolaides, K. H.** (2011). Assisted conception and placental perfusion assessed by uterine artery Doppler at 11-13 weeks' gestation. *Hum. Reprod.* **26**, 1659-1664. doi:10.1093/humrep/der117

**Centers for Disease Control and Prevention**, **American Society for Reproductive Medicine** and **Society for Assisted Reproductive Technology**. (2017). *2015 Assisted Reproductive Technology National Summary Report*. Atlanta, GA. US Dept of Health and Human Services.

**Chen, S., Sun, F.-Z., Huang, X., Wang, X., Tang, N., Zhu, B. and Li, B.** (2015a). Assisted reproduction causes placental maldevelopment and dysfunction linked to reduced fetal weight in mice. *Sci. Rep.* **5**, 10596. doi:10.1038/srep10596

**Chen, Z., Hagen, D. E., Elsik, C. G., Ji, T., Morris, C. J., Moon, L. E. and Rivera, R. M.** (2015b). Characterization of global loss of imprinting in fetal overgrowth syndrome induced by assisted reproduction. *Proc. Natl. Acad. Sci. USA* **112**, 4618-4623. doi:10.1073/pnas.1422088112

**Choux, C., Ginod, P., Barberet, J., Rousseau, T., Bruno, C., Sagot, P., Astruc, K. and Fauque, P.** (2019). Placental volume and other first-trimester outcomes: are there differences between fresh embryo transfer, frozen-thawed embryo transfer and natural conception? *Reprod. Biomed. Online* **38**, 538-548. doi:10.1016/j.rbmo.2018.12.023

**Coan, P. M., Conroy, N., Burton, G. J. and Ferguson-Smith, A. C.** (2006). Origin and characteristics of glycogen cells in the developing murine placenta. *Dev. Dyn.* **235**, 3280-3294. doi:10.1002/dvdy.20981

**Collier, A. C., Miyagi, S. J., Yamauchi, Y. and Ward, M. A.** (2009). Assisted reproduction technologies impair placental steroid metabolism. *J. Steroid Biochem. Mol. Biol.* **116**, 21-28. doi:10.1016/j.jsbmb.2009.04.005

**Conway, D. A., Liem, J., Patel, S., Fan, K. J., Williams, J. and Pisarska, M. D.** (2011). The effect of infertility and assisted reproduction on first-trimester placental and fetal development. *Fertil. Steril.* **95**, 1801-1804. doi:10.1016/j.fertnstert.2010.12.010

**Côté, A., Maheux-Lacroix, S., Sabr, Y., Gasse, C., Bujold, E. and Boutin, A.** (2019). Association between fertility treatments and early placentation markers. *Placenta* **82**, 35-41. doi:10.1016/j.placenta.2019.05.010

**Daniel, Y., Schreiber, L., Geva, E., Amit, A., Pausner, D., Kupferminc, M. J. and Lessing, J. B.** (1999). Do placentae of term singleton pregnancies obtained by assisted reproductive technologies differ from those of spontaneously conceived pregnancies? *Hum. Reprod.* **14**, 1107-1110. doi:10.1093/humrep/14.4.1107

**de Waal, E., Yamazaki, Y., Ingale, P., Bartolomei, M., Yanagimachi, R. and McCarrey, J. R.** (2012). Primary epimutations introduced during intracytoplasmic sperm injection (ICSI) are corrected by germline-specific epigenetic reprogramming. *Proc. Natl. Acad. Sci. USA* **109**, 4163-4168. doi:10.1073/pnas.1201990109

**de Waal, E., Mak, W., Calhoun, S., Stein, P., Ord, T., Krapp, C., Coutifaris, C., Schultz, R. M. and Bartolomei, M. S.** (2014). In vitro culture increases the frequency of stochastic epigenetic errors at imprinted genes in placental tissues from mouse concepti produced through assisted reproductive technologies. *Biol. Reprod.* **90**, 1-12. doi:10.1095/biolreprod.113.114785

**de Waal, E., Vrooman, L. A., Fischer, E., Ord, T., Mainigi, M. A., Coutifaris, C., Schultz, R. M. and Bartolomei, M. S.** (2015). The cumulative effect of assisted reproduction procedures on placental development and epigenetic perturbations in a mouse model. *Hum. Mol. Genet.* **24**, 6975-6985. doi:10.1093/hmg/ddv400

**Di Tommaso, M., Sisti, G., Colombi, I., Seravalli, V., Magro Malosso, E. R., Vannuccini, S. and Petraglia, F.** (2019). Influence of assisted reproductive technologies on maternal and neonatal outcomes in early preterm deliveries. *J. Gynecol. Obstet. Hum. Reprod.* **48**, 845-848. doi:10.1016/j.jogoh.2019.03.008

**Doherty, A. S., Mann, M. R. W., Tremblay, K. D., Bartolomei, M. S. and Schultz, R. M.** (2000). Differential effects of culture on imprinted H19 expression in the preimplantation mouse embryo. *Biol. Reprod.* **62**, 1526-1535. doi:10.1095/biolreprod62.6.1526

**Dumoulin, J. C., Land, J. A., Van Montfoort, A. P., Nelissen, E. C., Coonen, E., Derhaag, J. G., Schreurs, I. L., Dunselman, G. A., Kester, A. D., Geraedts, J. P. et al.** (2010). Effect of in vitro culture of human embryos on birthweight of newborns. *Hum. Reprod.* **25**, 605-612. doi:10.1093/humrep/dep456

**Dyer, S., Chambers, G. M., de Mouzon, J., Nygren, K. G., Zegers-Hochschild, F., Mansour, R., Ishihara, O., Banker, M. and Adamson, G. D.** (2016). International committee for monitoring assisted reproductive technologies world report: assisted reproductive technology 2008, 2009 and 2010. *Hum. Reprod.* **31**, 1588-1609. doi:10.1093/humrep/dew082

**Eindhoven, S. C., van Uitert, E. M., Laven, J. S. E., Willemsen, S. P., Koning, A. H. J., Eilers, P. H. C., Exalto, N., Steegers, E. A. P. and Steegers-Theunissen, R. P. M.** (2014). The influence of IVF/ICSI treatment on human embryonic growth trajectories. *Hum. Reprod.* **29**, 2628-2636. doi:10.1093/humrep/deu271

**Esh-Broder, E., Ariel, I., Abas-Bashir, N., Bdolah, Y. and Celnikier, D. H.** (2011). Placenta accreta is associated with IVF pregnancies: a retrospective chart review. *BJOG* **118**, 1084-1089. doi:10.1111/j.1471-0528.2011.02976.x

**Fauque, P., Jouannet, P., Lesaffre, C., Ripoche, M.-A., Dandolo, L., Vaiman, D. and Jammes, H.** (2007). Assisted Reproductive Technology affects developmental kinetics, H19 Imprinting Control Region methylation and H19

gene expression in individual mouse embryos. *BMC Dev. Biol.* **7**, 116. doi:10.1186/1471-213X-7-116

**Gagnon, R.** (2003). Placental insufficiency and its consequences. *Eur. J. Obstet. Gynecol. Reprod. Biol.* **110**, 99-107. doi:10.1016/S0301-2115(03)00179-9

**Haavaldsen, C., Tanbo, T. and Eskild, A.** (2012). Placental weight in singleton pregnancies with and without assisted reproductive technology: a population study of 536,567 pregnancies. *Hum. Reprod.* **27**, 576-582. doi:10.1093/humrep/der428

**Hwang, S. S., Dukhovny, D., Gopal, D., Cabral, H., Missmer, S., Diop, H., Declercq, E. and Stern, J. E.** (2018). Health of infants after ART-treated, subfertile, and fertile deliveries. *Pediatrics* **142**, e20174069. doi:10.1542/peds.2017-4069

**John, R. M.** (2013). Epigenetic regulation of placental endocrine lineages and complications of pregnancy. *Biochem. Soc. Trans.* **41**, 701-709. doi:10.1042/BST20130002

**Joy, J., Gannon, C., McClure, N. and Cooke, I.** (2012). Is assisted reproduction associated with abnormal placentation? *Pediatr. Dev. Pathol.* **15**, 306-314. doi:10.2350/11-11-1115-OA.1

**Joy, J., Armstrong, L., Ardill, J., Mcclure, N. and Cooke, I.** (2015). Biochemical markers of placental dysfunction in assisted conception. *Hum. Fertil. (Camb).* **18**, 282-290. doi:10.3109/14647273.2015.1083620

**Kaser, D. J., Melamed, A., Bormann, C. L., Myers, D. E., Missmer, S. A., Walsh, B. W., Racowsky, C. and Carusi, D. A.** (2015). Cryopreserved embryo transfer is an independent risk factor for placenta accreta. *Fertil. Steril.* **103**, 1176-1184.e2. doi:10.1016/j.fertnstert.2015.01.021

**Kobayashi, H., Hiura, H., John, R. M., Sato, A., Otsu, E., Kobayashi, N., Suzuki, R., Suzuki, F., Hayashi, C., Utsunomiya, T. et al.** (2009). DNA methylation errors at imprinted loci after assisted conception originate in the parental sperm. *Eur. J. Hum. Genet.* **17**, 1582-1591. doi:10.1038/ejhg.2009.68

**Lee, M. S., Cantonwine, D., Little, S. E., McElrath, T. F., Parry, S. I., Lim, K.-H. and Wilkins-Haug, L. E.** (2015). Angiogenic markers in pregnancies conceived through in vitro fertilization. *Am. J. Obstet. Gynecol.* **213**, 212.e1-212.e8. doi:10.1016/j.ajog.2015.03.032

**Luke, B., Brown, M. B., Wantman, E., Stern, J. E., Toner, J. P. and Coddington, C. C.** (2017). Increased risk of large-for-gestational age birthweight in singleton siblings conceived with in vitro fertilization in frozen versus fresh cycles. *J. Assist. Reprod. Genet.* **34**, 191-200. doi:10.1007/s10815-016-0850-x

**Luke, B., Brown, M. B., Eisenberg, M. L., Callan, C., Botting, B. J., Pacey, A., Sutcliffe, A. G. and Baker, V. L.** (2019). In vitro fertilization and risk for hypertensive disorders of pregnancy: associations with treatment parameters. *Am. J. Obstet. Gynecol.* **222**, P350.E1-P350.E13. doi:10.1016/j.ajog.2019.10.003

**Mainigi, M. A., Olalere, D. and Burd, I.** (2013). Peri-implantation hormonal milieu: elucidating mechanisms of abnormal placentation and fetal growth. *Biol. Reprod.* **90**, 1-9. doi:10.1095/biolreprod.113.110411

**Maltepe, E. and Fisher, S. J.** (2015). Placenta: the forgotten organ. *Annu. Rev. Cell Dev. Biol.* **31**, 523-552. doi:10.1146/annurev-cellbio-100814-125620

**Mann, M. R. W., Lee, S. S., Doherty, A. S., Verona, R. I., Nolen, L. D., Schultz, R. M. and Bartolomei, M. S.** (2004). Selective loss of imprinting in the placenta following preimplantation development in culture. *Development* **131**, 3727-3735. doi:10.1242/dev.01241

**Marino, J. L., Moore, V. M., Willson, K. J., Rumbold, A., Whitrow, M. J., Giles, L. C. and Davies, M. J.** (2014). Perinatal outcomes by mode of assisted conception and sub-fertility in an Australian data linkage cohort. *PLoS ONE* **9**, e80398. doi:10.1371/journal.pone.0080398

**Maynard, S. E., Min, J.-Y., Merchan, J., Lim, K.-H., Li, J., Mondal, S., Libermann, T. A., Morgan, J. P., Sellke, F. W., Stillman, I. E. et al.** (2003). Excess placental soluble fms-like tyrosine kinase 1 (sFlt1) may contribute to endothelial dysfunction, hypertension, and proteinuria in preeclampsia. *J. Clin. Invest.* **111**, 649-658. doi:10.1172/JCI17189

**Menelaou, K., Prater, M., Tunster, S. J., Blake, G. E. T., Joo, C. G., Cross, J. C., Hamilton, R. S. and Watson, E. D.** (2020). Blastocyst transfer in mice alters the placental transcriptome and growth. *Reproduction* **159**, 115-132. doi:10.1530/REP-19-0293

**Mu, J., Slevin, J. C., Qu, D., McCormick, S. and Adamson, S. L.** (2008). In vivo quantification of embryonic and placental growth during gestation in mice using micro-ultrasound. *Reprod. Biol. Endocrinol.* **6**, 34. doi:10.1186/1477-7827-6-34

**Nagy, A., Gertsenstein, M., Vintersten, K. and Behringer, R.** (2003). *Manipulating the Mouse Embryo: A Laboratory Manual*, 3rd edn. Cold Spring Harbor, NY: Cold Spring Harbor Laboratory Press.

**Nelissen, E. C., Van Montfoort, A. P., Coonen, E., Derhaag, J. G., Geraedts, J. P., Smits, L. J., Land, J. A., Evers, J. L. and Dumoulin, J. C.** (2012). Further evidence that culture media affect perinatal outcome: findings after transfer of fresh and cryopreserved embryos. *Hum. Reprod.* **27**, 1966-1976. doi:10.1093/humrep/des145

**Nelissen, E. C. M., Dumoulin, J. C. M., Daunay, A., Evers, J. L. H., Tost, J. and van Montfoort, A. P. A.** (2013). Placentas from pregnancies conceived by IVF/ICSI have a reduced DNA methylation level at the H19 and MEST differentially methylated regions. *Hum. Reprod.* **28**, 1117-1126. doi:10.1093/humrep/des459

**Outhwaite, J. E., McGuire, V. and Simmons, D. G.** (2015). Genetic ablation of placental sinusoidal trophoblast giant cells causes fetal growth restriction and embryonic lethality. *Placenta* **36**, 951-955. doi:10.1016/j.placenta.2015.05.013

**Palmer, K. R., Tong, S. and Kaitu'u-Lino, T. J.** (2016). Placental-specific sFLT-1: role in pre-eclamptic pathophysiology and its translational possibilities for clinical prediction and diagnosis. *Mol. Hum. Reprod.* **23**, 69-78. doi:10.1093/molehr/gaw077

**Pandey, S., Shetty, A., Hamilton, M., Bhattacharya, S. and Maheshwari, A.** (2012). Obstetric and perinatal outcomes in singleton pregnancies resulting from IVF/ICSI: a systematic review and meta-analysis. *Hum. Reprod. Update* **18**, 485-503. doi:10.1093/humupd/dms018

**Parchem, J. G., Kanasaki, K., Kanasaki, M., Sugimoto, H., Xie, L., Hamano, Y., Lee, S. B., Gattone, V. H., Parry, S., Strauss, J. F. et al.** (2018). Loss of placental growth factor ameliorates maternal hypertension and preeclampsia in mice. *J. Clin. Invest.* **128**, 5008-5017. doi:10.1172/JCI99026

**Petrussa, L., Van de Velde, H. and De Rycke, M.** (2014). Dynamic regulation of DNA methyltransferases in human oocytes and preimplantation embryos after assisted reproductive technologies. *Mol. Hum. Reprod.* **20**, 861-874. doi:10.1093/molehr/gau049

**Rahimi, S., Martel, J., Karahan, G., Angle, C., Behan, N. A., Chan, D., MacFarlane, A. J. and Trasler, J. M.** (2019). Moderate maternal folic acid supplementation ameliorates adverse embryonic and epigenetic outcomes associated with assisted reproduction in a mouse model. *Hum. Reprod.* **34**, 851-862. doi:10.1093/humrep/dez036

**Rhon-Calderon, E. A., Vrooman, L. A., Riesche, L. and Bartolomei, M. S.** (2019). The effects of Assisted Reproductive Technologies on genomic imprinting in the placenta. *Placenta* **84**, 37-43. doi:10.1016/j.placenta.2019.02.013

**Rizzo, G., Aiello, E., Pietrolucci, M. E. and Arduini, D.** (2016). Are there differences in placental volume and uterine artery Doppler in pregnancies resulting from the transfer of fresh versus frozen-thawed embryos through in vitro fertilization. *Reprod. Sci.* **23**, 1381-1386. doi:10.1177/1933719116641765

**Salvaing, J., Peynot, N., Bedhane, M. N., Veniel, S., Pellier, E., Boulesteix, C., Beaujean, N., Daniel, N. and Duranthon, V.** (2016). Assessment of 'one-step' versus 'sequential' embryo culture conditions through embryonic genome methylation and hydroxymethylation changes. *Hum. Reprod.* **31**, 2471-2483. doi:10.1093/humrep/dew214

**Sanchez, O., Llurba, E., Marsal, G., Dominguez, C., Aulesa, C., Sanchez-Duran, M. A., Goya, M. M., Alijotas-Reig, J., Carreras, E. and Cabero, L.** (2012). First trimester serum angiogenic/anti-angiogenic status in twin pregnancies: relationship with assisted reproduction technology. *Hum. Reprod.* **27**, 358-365. doi:10.1093/humrep/der394

**SanMiguel, J. M., Abramowitz, L. K. and Bartolomei, M. S.** (2018). Imprinted gene dysregulation in a *Tet1* null mouse model is stochastic and variable in the germline and offspring. *Development* **145**, dev160622. doi:10.1242/dev.160622

**Schieve, L. A., Cohen, B., Nannini, A., Ferre, C., Reynolds, M. A., Zhang, Z., Jeng, G., Macaluso, M. and Wright, V. C.** (2007). A population-based study of maternal and perinatal outcomes associated with assisted reproductive technology in Massachusetts. *Matern. Child Health J.* **11**, 517-525. doi:10.1007/s10995-007-0202-7

**Simmons, D. G.** (2014). *The Guide to Investigation of Mouse Pregnancy*. Elsevier.

**Stern, J. E., Liu, C., Cabral, H. J., Richards, E. G., Coddington, C. C., Hwang, S., Dukhovny, D., Diop, H. and Missmer, S. A.** (2018). Birth outcomes of singleton vaginal deliveries to ART-treated, subfertile, and fertile primiparous women. *J. Assist. Reprod. Genet.* **35**, 1585-1593. doi:10.1007/s10815-018-1238-x

**Sui, L., An, L., Tan, K., Wang, Z., Wang, S., Miao, K., Ren, L., Tao, L., He, S., Yu, Y. et al.** (2014). Dynamic proteomic profiles of in vivo- and in vitro-produced mouse postimplantation extraembryonic tissues and placentas. *Biol. Reprod.* **91**, 1-16. doi:10.1095/biolreprod.114.124248

**Sundheimer, L. W., Chan, J. L., Buttle, R., DiPentino, R., Muramoto, O., Castellano, K., Wang, E. T., Williams, J. and Pisarska, M. D.** (2018). Mode of conception does not affect fetal or placental growth parameters or ratios in early gestation or at delivery. *J. Assist. Reprod. Genet.* **35**, 1039-1046. doi:10.1007/s10815-018-1176-7

**Tan, K., Zhang, Z., Miao, K., Yu, Y., Sui, L., Tian, J. and An, L.** (2016). Dynamic integrated analysis of DNA methylation and gene expression profiles in in vivo and in vitro fertilized mouse post-implantation extraembryonic and placental tissues. *Mol. Hum. Reprod.* **22**, 485-498. doi:10.1093/molehr/gaw028

**Thomopoulos, C., Salamalekis, G., Kintis, K., Andrianopoulou, I., Michalopoulou, H., Skalis, G., Archontakis, S., Argyri, O., Tsioufis, C., Makris, T. K. et al.** (2017). Risk of hypertensive disorders in pregnancy following assisted reproductive technology: overview and meta-analysis. *J. Clin. Hypertens.* **19**, 173-183. doi:10.1111/jch.12945

**Tunster, S. J., Jensen, A. B. and John, R. M.** (2013). Imprinted genes in mouse placental development and the regulation of fetal energy stores. *Reproduction* **145**, R117-R137. doi:10.1530/REP-12-0511

**Tunster, S. J., Boqué-Sastre, R., McNamara, G. I., Hunter, S. M., Creeth, H. D. J. and John, R. M.** (2018). Peg3 deficiency results in sexually dimorphic losses and gains in the normal repertoire of placental hormones. *Front. Cell Dev. Biol.* **6**, 123. doi:10.3389/fcell.2018.00123

**Vermey, B. G., Buchanan, A., Chambers, G. M., Kolibianakis, E. M., Bosdou, J., Chapman, M. G. and Venetis, C. A.** (2018). Are singleton pregnancies after assisted reproduction technology (ART) associated with a higher risk of placental anomalies compared with non-ART singleton pregnancies? A systematic review and meta-analysis. *BJOG* **126**, 209-218. doi:10.1111/1471-0528.15227

**von Versen-Höynck, F., Schaub, A. M., Chi, Y.-Y., Chiu, K.-H., Liu, J., Lingis, M., Stan Williams, R., Rhoton-Vlasak, A., Nichols, W. W., Fleischmann, R. R. et al.** (2019). Increased preeclampsia risk and reduced aortic compliance with in vitro fertilization cycles in the absence of a Corpus Luteum. *Hypertension* **73**, 640-649. doi:10.1161/HYPERTENSIONAHA.118.12043

**Whidden, L., Martel, J., Rahimi, S., Chaillet, J. R., Chan, D. and Trasler, J. M.** (2016). Compromised oocyte quality and assisted reproduction contribute to sex-specific effects on offspring outcomes and epigenetic patterning. *Hum. Mol. Genet.* **25**, 4649-4660. doi:10.1093/hmg/ddw293

**White, C. R., Denomme, M. M., Tekpetey, F. R., Feyles, V., Power, S. G. A. and Mann, M. R. W.** (2015). High frequency of imprinted methylation errors in human preimplantation embryos. *Sci. Rep.* **5**, 17311. doi:10.1038/srep17311

**Wisborg, K., Ingerslev, H. J. and Henriksen, T. B.** (2010). In vitro fertilization and preterm delivery, low birth weight, and admission to the neonatal intensive care unit: a prospective follow-up study. *Fertil. Steril.* **94**, 2102-2106. doi:10.1016/j.fertnstert.2010.01.014

**Woods, L., Perez-Garcia, V. and Hemberger, M.** (2018). Regulation of placental development and its impact on fetal growth-new insights from mouse models. *Front. Endocrinol. (Lausanne).* **9**, 570. doi:10.3389/fendo.2018.00570

**Zhang, Y., Zhao, W., Jiang, Y., Zhang, R., Wang, J., Li, C., Zhao, H., Gao, L., Cui, Y., Zhou, Z. et al.** (2011). Ultrastructural study on human placentae from women subjected to assisted reproductive technology treatments. *Biol. Reprod.* **85**, 635-642. doi:10.1095/biolreprod.110.090589